JNeurosci
THE JOURNAL OF NEUROSCIENCE

Research Articles: Neurobiology of Disease

Dopamine restores limbic memory loss, dendritic spine structure and NMDAR-dependent LTD in the nucleus accumbens of alcohol-withdrawn rats

Carla Cannizzaro[1], Giuseppe Talani[2], Anna Brancato[1], Giovanna Mulas[3], Saturnino Spiga[3], Maria Antonietta De Luca[4], Angela Sanna[5], Rosa Anna Maria Marino[6], Giovanni Biggio[2,3], Enrico Sanna[2,3] and Marco Diana[7]

[1]*Lab of Neuropsychopharmacology, Department ProSaMI "G. D'Alessandro", University of Palermo, Via del Vespro 129 90127, Palermo, Italy*

[2]*Institute of Neuroscience, National Research Council, 09042 Monserrato (CA), Italy.*

[3]*Department of Life and Environmental Sciences, Section of Neuroscience and Anthropology, University of Cagliari, 09042 Monserrato (CA) Italy.*

[4]*Department of Biomedical Sciences, Section of Neuropsychopharmacology, University of Cagliari, Cittadella Universitaria- S.P. Monserrato Sestu km 0.700, 09042 Monserrato (CA), Italy.*

[5]*Department of Medical Science and Public Health, University of Cagliari, Cittadella Universitaria- S.P. Monserrato Sestu km 0.700, 09042 Monserrato (CA), Italy.*

[6]*Intramural Research Program, National Institute on Drug Abuse, National Institutes of Health, Baltimore, MD 21224, USA.*

[7]*University of Sassari, 'G.Minardi' Laboratory of Cognitive Neuroscience, Department of Chemistry and Pharmacy Via Muroni, 23 07100 Sassari, Italy.*

https://doi.org/10.1523/JNEUROSCI.1377-18.2018

Received: 30 May 2018

Revised: 28 September 2018

Accepted: 15 October 2018

Published: 16 November 2018

Author contributions: C.C., G.T., A.B., G.M., and S.S. performed research; C.C., G.T., A.B., G.M., S.S., M.A.D.L., A.S., R.a.M.M., G.B., and E.S. analyzed data; C.C., E.S., and M.D. wrote the paper; G.T. and A.B. wrote the first draft of the paper; M.A.D.L., A.S., R.a.M.M., G.B., and E.S. contributed unpublished reagents/ analytic tools; M.D. designed research; M.D. edited the paper.

Conflict of Interest: The authors declare no competing financial interests.

We are grateful to the Fondazione Banco di Sardegna U1077.2015/AI.961.BE, CNR-DISVA-Sardegna Ricerche, Gieffe Supermercati and Region of Sicily - Department of Family, Social Policies and Job - for the In-dependent Generation grant.

Corresponding author : Marco Diana, MD, PhD, 'G.Minardi' Laboratory of Cognitive Neuroscience, University of Sassari, Department of Chemistry and Pharmacy, Via Muroni, 23 07100 Sassari, Italy., dsfdiana@uniss.it

Cite as: J. Neurosci 2018; 10.1523/JNEUROSCI.1377-18.2018

Title

Dopamine restores limbic memory loss, dendritic spine structure and NMDAR-dependent LTD in the nucleus accumbens of alcohol-withdrawn rats.

Abbreviated title

Dopamine-dependent limbic memory in alcohol dependence.

Author names and affiliation, including postal codes

Carla Cannizzaro[1*]; Giuseppe Talani[2*]; Anna Brancato[1]; Giovanna Mulas[3]; Saturnino Spiga[3]; Maria Antonietta De Luca[4], Angela Sanna[5], Rosa Anna Maria Marino[6], Giovanni Biggio[2,3]; Enrico Sanna[2,3] and Marco Diana[7]

[1]Lab of Neuropsychopharmacology, Department ProSaMI "G. D'Alessandro", University of Palermo, Via del Vespro 129 90127, Palermo, Italy; [2]Institute of Neuroscience, National Research Council, 09042 Monserrato (CA), Italy. [3]Department of Life and Environmental Sciences, Section of Neuroscience and Anthropology, University of Cagliari, 09042 Monserrato (CA) Italy. [4]Department of Biomedical Sciences, Section of Neuropsychopharmacology, University of Cagliari, Cittadella Universitaria- S.P. Monserrato Sestu km 0.700, 09042 Monserrato (CA), Italy. [5]Department of Medical Science and Public Health, University of Cagliari, Cittadella Universitaria- S.P. 19 Monserrato Sestu km 0.700, 09042 Monserrato (CA), Italy. [6]Intramural Research Program, National Institute on Drug Abuse, National Institutes of Health, Baltimore, MD 21224, USA. [7]University of Sassari, 'G.Minardi' Laboratory of Cognitive Neuroscience, Department of Chemistry and Pharmacy Via Muroni, 23 07100 Sassari, Italy.

*** Drs. Cannizzaro and Talani contributed equally to this work.**

Corresponding author

Marco Diana, MD, PhD

'G.Minardi' Laboratory of Cognitive Neuroscience

University of Sassari, Department of Chemistry and Pharmacy

Via Muroni, 23 07100 Sassari, Italy.

dsfdiana@uniss.it

Number of pages = 48

Number of figures = 8, tables = 2, multimedia and 3D models (0)

Number of words for Abstract = 193, Introduction = 644, and Discussion = 1635

Conflict of Interest: The authors declare no competing financial interests.

Acknowledgements:

We are grateful to the Fondazione Banco di Sardegna U1077.2015/AI.961.BE, CNR-DISVA-Sardegna Ricerche, Gieffe Supermercati and Region of Sicily - Department of Family, Social Policies and Job - for the In-dependent Generation grant.

Abstract

Alcohol abuse leads to aberrant forms of emotionally salient memory - i.e. limbic memory - that promote escalated alcohol consumption and relapse. Accordingly, activity-dependent structural abnormalities, are likely to contribute to synaptic dysfunctions that occur from suddenly ceasing chronic alcohol consumption. Here we show that alcohol dependent male rats fail to perform an emotional-learning task during abstinence but recover their functioning by L-DOPA administration during early withdrawal. L-DOPA also reverses the selective loss of dendritic “long thin” spines observed in medium spiny neurons of the nucleus accumbens (NAc) shell of alcohol-dependent rats during abstinence, as well as the reduction in tyrosine hydroxylase (TH) immunostaining and postsynaptic density-95 (PSD-95)-positive elements. Patch-clamp experiments in NAc slices reveal that both *in-vivo* systemic L-DOPA administration and *in-vitro* exposure to dopamine can restore the loss of long-term depression (LTD) formation, counteract the reduction in NMDAR-mediated synaptic currents and rectify the altered NMDAR/AMPAR ratio observed in alcohol-withdrawn rats. Further, *in-vivo* microdialysis experiments show that blunted dopaminergic signaling is revived after L-DOPA treatment during early withdrawal. These results suggest a key role of an efficient dopamine signaling for maintaining – and restore - neural trophism, NMDA-dependent LTD and ultimately optimal learning.

Significance Statement

Blunted dopamine signaling and altered glutamate connectivity in the nucleus accumbens represent the neuroanatomical basis for the impairment in aversive limbic memory observed during withdrawal in alcohol dependence. Supplying L-DOPA during withdrawal re-establishes synaptic morphology and functional neuroadaptations, suggesting a complete recovery of nucleus accumbens glutamatergic synaptic plasticity

when dopamine is revived. Importantly, restoring dopamine transmission allows those synapses to encode emotionally relevant information and rescue flexibility in the neuronal circuits that process limbic memory formation. Under these conditions, drugs capable of selectively boosting the dopaminergic function during the “fluid” and still responsive state of the early withdrawn maladaptive synapses may help in the treatment of alcohol addiction.

Introduction

Alcohol withdrawal is associated with a series of negative affective symptoms whose occurrence, as negative reinforcement, increases the motivation for relapse and, in turn, favors the maintenance of addiction (Koob and LeMoal, 2001; Heilig et al., 2010). A substantial body of work indicates that aberrant dopaminergic (DAergic) and glutamatergic-based plasticity in the mesocorticolimbic reward system plays a critical role in alcohol addiction and relapse (Koob and Volkow, 2010).

As a key component of the reward circuitry, the nucleus accumbens (NAc) is critical in the development of addiction. It receives DAergic signaling from the ventral tegmental area (VTA), as well as robust glutamatergic innervations from prefrontal cortex, hippocampus, amygdala, and the thalamus, converging on a common postsynaptic target, the striatal medium spiny neuron (MSN). Here, dendritic spines show a peculiar synaptic arrangement, called the “striatal microcircuit” or “synaptic triad” (Freund et al., 1984; Carr and Sesack, 1996). Alcohol dependence may affect the plasticity in the NAc synaptic triad architecture (Hyman et al., 2006; Gass and Olive, 2008; Kalivas and Volkow, 2011; Kauer and Malenka, 2007) including changes in density and head size of dendritic spines (Zhou et al., 2007; Uys et al., 2016). Accordingly, previous research had found signs of aberrant plasticity on MSNs of alcohol-withdrawn rats, evidenced by the simultaneous visualization of reduced DAergic projections (tyrosine hydroxylase, TH), post-synaptic density scaffold (PSD-95), and the selective remodeling of dendritic spine architecture (Spiga et al., 2014). Such changes are in agreement with a reduction in VTA DAergic firing rate in withdrawn rats (Rothblat et al., 2001; Diana et al., 1993) and strengthen the view of a link between synaptic indices of remodeling and the dampening in dopamine (DA) signaling (Diana et al., 1993; Weiss et al., 1996). Further, recent works (Berry and Nedivi, 2017; Bosch et al., 2014; Kasai et al., 2010, Lendvai et al., 2000) suggest a potential relationship between spine shape’s rearrangement and synaptic dynamic response, as forms of experience-

dependent plasticity (Trachtenberg et al., 2002) underpinning cellular learning (Bourne and Harris, 2007). Hence, the molecular, neuronal and structural changes occurring during the development of addiction share similarities with those of physiological learning (Kiefer and Dinter, 2013). Moreover, the brain reward regions (VTA and NAc) potently influence behavioral memory through a direct involvement of DA neurons (Nestler, 2013). Indeed, DA neurons undergo experience-dependent synaptic plasticity during aversive experiences presumably by adding specific emotional weight and play a main role in the early stabilization of the memory trace of fear-related learning (Pignatelli et al., 2017). Accordingly, recovery of DA signaling in the striatum of DA-deficient mice was necessary to enable them to learn two-way active avoidance, by restoring synaptic strength (Darvas et al., 2011). Notably persistent impairment in synaptic strength, such as occluded long-term depression (LTD), could explain the loss of control on alcohol intake and relapse observed in addicted rodents (Ma et al., 2018). Putting the puzzle together, alcohol dependence, by dampening DAergic transmission, hijacks synaptic plasticity rules in the striatal network, and this can result in aberrant forms of emotionally salient memory- i.e. limbic memory- that may promote alcohol dependence. It follows that if we could rectify the alterations in the neuronal network connectivity associated to alcohol withdrawal, we would restore adaptive forms of functional and behavioral plasticity. This compelling theory was challenged by the present investigation, which focuses on the impact of a restored DA signaling upon the morphological, functional and behavioral correlates of alcohol withdrawal. In particular, by employing an integrated strategy of investigation we assessed: aversive limbic memory as a distinctive form of emotional memory; spine density and morphology in NAc MSNs; immunoreactivity for both TH and PSD-95; long-term plasticity at the striatal post-synaptic component; DA levels in the NAc by in vivo microdialysis; the putative recovery effect of acute L-DOPA treatment during withdrawal.

The possibility that boosting DA signaling may lead to a rescue of alcohol-related dysfunction suggests therapeutic implications.

Materials and Methods

Animals

Male Sprague-Dawley rats (Charles River, Italy), weighing 125-155 g at the beginning of treatment, were housed individually in single cages. No extra chow or water was supplied and animals were fed only with a liquid diet, continuously available, prepared as previously reported (Spiga et al., 2014). Briefly, fresh whole cow milk, 910-970 ml (CoaPla, Italy), vitamin A 5000 IU/l and sucrose 17 g/l that supplies 1000.7 kcal/l, was freshly prepared daily. Temperature 22 ± 2 °C and humidity 60-65% were maintained under controlled environmental conditions (on a reverse 12-h light/dark cycle). Animals were divided in different experimental groups: alcohol-naïve controls (CTRL, continuously fed with alcohol-free milk); chronically alcohol-treated rats (EtOH-CHR, continuously fed with alcohol-containing milk and tested immediately after treatment was terminated); alcohol withdrawn rats (EtOH-WDL, continuously fed with alcohol-containing milk and tested 12 h after treatment was terminated); EtOH-WDL(48 h) - and EtOH-WDL(14 d)-rats tested respectively 48 hours and 14 days following the interruption of the chronic alcohol diet. All experiments were conducted in accordance with the regulations of the Committee for the Protection and Use of Animals of the University of Palermo, Sassari and Cagliari, in accordance with current Italian legislation on animal experimentation (D.L. 26/2014) and the European directives (2010/63/EU) on care and use of laboratory animals (authorization no. 172/2017-PR to E.S.). Every effort was made to minimize the number of animals used and their sorrow.

153 **Experimental design**

154 Details of the experiments, groups, factors and analysis employed are displayed in table 1.

155

156 **Alcohol dependence induction**

157 Alcohol dependence was induced by feeding rats with a liquid diet as previously
158 reported (Spiga et al., 2014). Briefly, the mix was presented at the same time of the day
159 (09:30 AM). The diet was gradually enriched with 2.4% (days 1-4), 4.8% (days 5-8) and
160 7.2% (days 9-20) alcohol and administered for 20 days. The animal body weight, as well
161 as alcohol and liquid intake, were monitored daily. Under these experimental conditions
162 blood alcohol concentrations reach 76.41 ± 16.41 mg/dL within 30 min of liquid diet
163 suspension; and <1 mg/dL at 12 h after liquid diet suspension (EtOH-WDL rats) (Spiga et
164 al., 2014).
165 Controls (CTRL) were pair-fed with alcohol-free milk liquid diet.
166 Withdrawal signs, including body tremors, tail stiffness; irritability to touch (vocalization)
167 were monitored and scored by a skilled experimenter blind to treatments using a rating
168 scale as follows: 0 = no sign, 1 = moderate, 2 = severe (see Spiga et al., 2014). Individual
169 withdrawal sign rating was then combined to produce a global score of withdrawal severity
170 with a maximum total of 6.

171

172 **Emotional-Object Recognition (EOR) test**

173 Apparatus

174 The EOR test was used for the assessment of aversive limbic memory. It employed
175 two distinct contexts (A and B) placed in different rooms. Context “A chamber” is a
176 rectangular arena with white floors (100 long x 30 wide x 43 high cm). Rat behavior was
177 recorded and analyzed by ANY MAZE Video Tracking System (Ugo Basile, Italy). A left
178 and a right zone (40 x 30 cm) on both ends of Context “A chamber”, as well as a neutral

zone in the centre of the box (20 cm) represented the arena settings (modified from Ramirez et al., 2015). Context “A chamber” was customized with two different, non-toxic objects (i.e. a plastic ball, 3.5 cm diameter, and a plastic pepper, 3 x 3 x 4 cm) that were placed against the end walls of the left and the right zones of the arena, according to the procedure described below. Objects and their position were counter-balanced within the experimental groups.

Context “B chamber” was a rectangular chamber (45 x 22 x 22 cm), and equipped with grid floor, opaque ceilings and dark walls. Rats were allowed to explore Context “B chamber” for habituation and conditioned/cued-learning; they were then tested in Context “A chamber” for emotional recognition. Floors and walls of the chambers were thoroughly cleaned with 70% isopropanol, then dried with tissue paper, and rinsed again with water 10 min before animals’ entry into the chambers. Rats were transported to and from the experimental room in their home cages using a wheeled cart. The cart and cages remained in an anteroom to the experimental rooms during all behavioral experiments.

Experimental design (Fig 1a)

Habituation

Habituation took place in Context “B chamber” and consisted of two separate sessions: environmental exploration, during which rats were put in the arena and left undisturbed to explore the chamber for 5 min; neutral-object exploration, in which an object (plastic ball or pepper) was placed in the opposite corner with respect to the rat's entry and presented to the animals for 10 min. Between the two sessions, rats were taken and returned to their home cages for 10 minutes.

Cued Fear-conditioned Learning

1h after neutral-object exploration, rats were re-placed in Context “B chamber”,

presented with a novel object (emotional-object)-and trained for fear conditioning. The session was 560 s in duration, and five 2 s - 0.3 mA shocks were delivered at 120 s, 200 s, 280 s, 360 s, 440 s and 520 s. At the end of the session, animals returned in their home cages for 4 h retention interval.

Emotional-Object Recognition - Context A chamber

Four hours after cued-fear conditioned learning, animals were put into Context “A chamber” and tested for emotional-object discrimination and object-place aversion in a neutral context, “A chamber”. They were allowed to freely explore the new context for 5 min; for each rat, favorite zone, between left and right ones, was recorded at epoch baseline (BSL). Afterwards, the object experienced during fear conditioning (emotional object) - was placed in the favorite zone; the object experienced during habituation (neutral- object) was placed in the less preferred zone. Rats explored objects and zones from minutes 5 to 8 (epoch ON-1). During minutes 8–11, objects were removed from the arena (epoch OFF). During minutes 11 to 14, the objects were reintroduced in the same positions as minutes 5–8 (epoch ON-2). Finally, rats were placed in their home cages and carted back to the holding room. At the end of each experimental session, both objects and arena were cleaned with a 70% solution of isopropanol. Time spent on exploring objects and zones was recorded along the epochs. Emotional-object discrimination was measured by “emotional-object avoidance %”, which was calculated as: 100 - [(time spent on the emotional-object / time spent on neutral + emotional-object) %)]. Object-place conditioning was measured by "Target-zone aversion score “, which was calculated as the difference between time spent on the target zone during BSL and the mean time spent on the target zone during ON epochs.

Drugs (behavior)

L-DOPA was used at the dose of 6 mg/kg (Nikolaus et al., 2016) in all the experimental procedures; the dose of 1.5 mg/kg was also tested in the aversive limbic-memory experiment. L-DOPA was administered by a subcutaneous single injection 1h before the cued fear-conditioned learning session. In addition, in order to prevent the peripheral decarboxylation of DOPA, the DOPA decarboxylase inhibitor benserazide (6 mg/kg) was co-injected. Control rats received the same volume of vehicle (1 ml/kg), at the same time schedule.

Locomotor activity

Locomotor activity was measured in the context “A chamber”, during the 5 min-epoch baseline (BSL) of the emotional object recognition experiment. The motor pattern of the rats was recorded by employing an automatic video-tracking system (ANY MAZE, Ugo Basile, Italy), and measured as total distance travelled (m, TDT).

Hot-water immersion- tail flick test

Nociception was explored by measuring tail-flick latencies in the “hot-water immersion- tail flick” test, following the emotional object recognition test. Rats' tail was immersed for 2 cm in a water bath apparatus (Instruments srl, Bernareggio, MI, Italy) maintained at 52 ± 0.5° C. Latency to response was determined by a vigorous tail flick by a skilled experimenter blind to treatments. A cut-off time of 10 s was imposed to minimize tissue damage.

Golgi-Cox and simultaneous immunofluorescence

Rats were deeply anesthetized with chloral hydrate and perfused intracardially with 0.9% saline solution (400 ml) followed by 4% paraformaldehyde (pH 7.4) (200 ml). The removed brains were post fixed in same fixative overnight at 4 C°. Afterwards brains were

washed in 0.4 M Sorenson's Phosphate Buffer (PBS) for 8 h (eight change of one hour each) and placed in 20 ml of Golgi-Cox solution for two weeks. Brains were cut in 50 µm thick coronal slices using a vibratome Leica VT 1000S. Slices were developed in ammonia solution at 15% for 30min (Spiga et al., 2014), washed and collected in PBS for the following free-floating immunostaining. To prevent non-specific binding, slices were pre-incubated in 10% normal goat serum (NGS) solution containing 5% bovine serum albumin (BSA) and 1% Triton X-100 in PBS overnight at 4 C°. At this point, sections were incubated with two primary antibodies: polyclonal rabbit anti-TH (Santa Cruz Biotechnology, Inc) (1:200) and mouse anti PSD-95 (Santa Cruz Biotechnology, Inc.) (1:200) in PBS for 48 h at 4° C.

Sections were washed 3 x 10 min in PBS, and incubated in biotinylated goat anti-mouse (Vector Laboratories, Burlingame, CA) (1:200), and anti-rabbit Alexa Fluor 594 (Molecular Probes) (1:200), in PBS for 4h at RT. After this step, slices were incubated in Fluorescein-Streptavidin (Vector Laboratories, Burlingame, CA) (1:200) in PBS for 1h at RT and then washed 3 X 10 min in PBS and coverslipped with Vectashield (Vector Laboratories, Burlingame, CA).

TH, PSD-95 counts

For counts, confocal images were obtained 24h after the conclusion of the histology procedure. The TH and PSD-95 volume were determined as follow:

For each dataset (n = 6 - 8 rats per group), four surfaces (x= 40 µm; y= 40 µm; z=10) (ROI) were randomly chosen by an experimenter blind to treatments. In each ROI, by a simple thresholding, objects were created and their volume was calculated, summed and expressed as volume/μm^3.

Spines density and classification

For spines density evaluation, n=40 distal dendritic segments (at least 20 µm long), from confocal images of shell MSN of each experimental group (n = 6 - 8 rats per group), were collected and automatically (filament tool Bitplane Imaris 7.4) counted. Using the same dendritic segment, we classified spine typology according to Spiga et al., 2014.

Laser scanning confocal microscopy

Confocal analysis was performed using a Leica 4D confocal laser-scanning microscope with an argon–krypton laser. Confocal images were generated using 100X oil (n.a. 1.3). Each frame was acquired eight times and then averaged to obtain noise-free images. Scans were performed in sequence using channels for fluorescein, rhodamine and reflection, using, exactly, the same range in Z axis. Resulting datasets were combined, frame by frame, for simultaneous rendering.

Rendering

Maximum intensity and Extended focus algorithms were used for surface rendering to display and analyze the anatomical structures. The rendered 3D surfaces were analyzed for counts and to show the interaction between fluorescence and Golgi-Cox stained elements. Colocalization analysis (Imaris 7.0) was also used.

Electrophysiology experiments

Coronal brain slices containing the NAc shell region were prepared as previously described (Spiga et al., 2014). Briefly, animals were subjected to deep anesthesia with isoflurane 2-5% and decapitated. Their brain was rapidly removed from the skull and transferred to a modified artificial cerebrospinal fluid (ACSF) containing (in mM): 220 sucrose, 2 KCl, 0.2 $CaCl_2$, 6 $MgSO_4$, 26 $NaHCO_3$, 1.3 NaH_2PO_4, and 10 D-glucose (pH 7.4, set by aeration with 95% O_2 and 5% CO_2). Coronal brain slices (thickness, 260 µm)

containing the NAc shell were cut in ice-cold modified ACSF with the use of a Leica VT1200S vibratome (Leica, Heidelberg, Germany). Slices were then transferred immediately to a nylon net submerged in standard ACSF containing (in mM): 126 NaCl, 3 KCl, 2 CaCl2, 1 MgCl2, 26 NaHCO3, 1.25 NaH2PO4, and 10 D-glucose (pH 7.4, set by aeration with 95% O2/5% CO2) for at least 40 min at a controlled temperature of 35°C. After subsequent incubation for at least 1h at room temperature, hemi-slices were transferred to the recording chamber, and continuously perfused with standard ACSF at a constant flow rate of ~2 ml/min. For all recordings, the temperature of the bath was maintained at 33°C. Glutammatergic excitatory postsynaptic currents (EPSCs) were recorded, in the presence of the GABAA receptor antagonist bicuculline (20 μM), with an Axopatch 200-B amplifier, filtered at 2 kHz, and digitized at 5 kHz. For evoked EPSCs a bipolar concentric stimulating electrode was placed at the bottom of the NAc shell while recorded MSNs were always located about 400 μm above the stimulating electrode tip. For calculating the NMDA/AMPA ratio, AMPAr-mediated eEPSCs were recorded at a holding potential of -65 mV, while NMDAr-mediated responses were recorded at a holding potential of +40 mV in the presence of the AMPA/kainate receptor antagonist CNQX (5 μM). For LTD experiments, eEPSCs were recorded in voltage-clamped (-65 mV) MSNs at a frequency of 0.05 Hz (baseline) for at least 10 min; no differences were found in baseline currents at the stimulation used to evoke the 30% of maximal response; a low frequency stimulation (LFS, 500 stimuli at 1 Hz) paired with membrane depolarization (holding potential, -50 mV) was then applied, and eEPSCs were then recorded for the following 60 min at a frequency stimulation of 0.05 Hz. LTD was calculated by averaging the EPSC amplitude values measured 50 to 60 min after LFS and expressed as percentage of baseline as average of the last 10 min of recording.

Drugs (electrophysiology)

L-3,4-dihydroxyphenylalanin (L-DOPA, 6 mg/kg) was administered acutely by a subcutaneous injection 1h before sacrifice, in association with the peripheral antagonist of DOPA decarboxylase, benserazide (6 mg/kg). Moreover, the following drugs were tested "in vitro" by bath perfusion of NAc slices, obtained from the different experimental groups, for 5 min before applying LFS: dopamine (10 µM), the D1R antagonist SCH23390 (10 µM), and the D2R antagonist sulpiride (10 µM).

In vivo microdialysis studies

Rats were anesthetized with Equitesin (3 ml/kg ip), and placed in a stereotaxic apparatus. The skull was exposed, and a small hole was drilled on one side. The probe was implanted vertically in the NAc shell (A + 2.2; L + 1.0 from bregma; V-7.8 from dura) according to Paxinos and Watson (1998), and then fixed on the skull with dental cement. Rats were housed in transparent plastic (Plexiglas) hemispheric bowls with liquid diet available. Experiments were performed on freely moving rats 24 h after probe implantation. A Ringer's solution (147 mM, NaCl; 2.2 mM, CaCl2; 4 mM, KCl) was pumped through the dialysis probe at a constant rate of 1 µl/min. Dialysate samples (20 µl) were taken every 20 min and injected without purification into an HPLC apparatus equipped with a reverse-phase column (C8 3.5 µm, Waters, Mildford, MA, USA) and a coulometric detector (ESA Coulochem II, Bedford, MA, USA) to quantify DA. The first electrode of the detector was set at + 130 mV (oxidation) and the second at −175 mV (reduction). The composition of the mobile phase was 50 mM NaH2PO4, 0.1 mM Na2-EDTA, 0.5 mM n-octyl sodium sulfate, and 15% (v/v) methanol, pH 5.5. The sensitivity of the assay for DA was 5 fmol/sample. At the end of the experiment, animals were sacrificed and their brains were removed and stored in formalin (8%) before histological analysis. To this end, brains were cut on a vibratome in serial coronal slices (20 µm) oriented according to Paxinos and Watson (1998) to locate the placement of the microdialysis probe.

361

362 **Statistical Analysis**

363 All data are expressed as the mean ± SEM, unless differently indicated. All data
364 were tested for normality and equal variances. When data exhibit normality and equal
365 variances, differences between groups were determined using either a one– or two–way
366 analysis of variance (ANOVA) followed by Bonferroni post hoc test when the main effect
367 was significant ($p<0.05$). Data from in vivo microdialysis were analysed by utilizing
368 repeated measures two-way ANOVA (RM two-way ANOVA), followed by post hoc Sidak or
369 Tukey tests, when necessary. Data that did not display equal variances and data from the
370 withdrawal rating scale were analyzed by Kruskal-Wallis, followed by Dunn's post hoc test
371 when necessary and Mann-Whitney U- nonparametric tests.
372 Statistical analysis was performed using Prism 6.0 (GraphPad Software, La Jolla,
373 California). No statistical methods were used to predetermine sample sizes but our sample
374 sizes are similar to those reported in previous publications. Grubbs outlier test was
375 performed on immunofluorescence images that varied > 2 SDs from the mean were
376 removed and not considered for data analysis (one image out of eight for two samples out
377 of six in CTRL group; one image out of eight for two samples out of eight of EtOH-WDL
378 and EtOH-WDL+ L-DOPA groups).

379

380 **Results**

381 **Signs of withdrawal from ethanol liquid diet administration**

382 The signs of withdrawal at 12 h, 48 h, and 14 days after EtOH diet suspension were
383 scored immediately before the EOR testing in the different experimental groups. Each
384 individual sign of withdrawal was rated on a 0-2-point scale; then they were combined to
385 produce a global score of withdrawal severity with a maximum total of 6 (Table 2). Data
386 analysis on global score rating, including withdrawal as main factor, revealed significant

differences among the groups [Kruskal-Wallis statistic = 27.84, $p < 0.001$]. In particular, withdrawal global score was significantly higher in rats at 12 h withdrawal from EtOH liquid diet than controls [$p < 0.001$, Dunn's multiple comparisons test] and 48 h [$p = 0.0224$, Dunn's multiple comparisons test] time points, while no differences were observed at 14 d [$p > 0.999$, Dunn's multiple comparisons test]. The analysis of individual signs of withdrawal indicated significant differences in body tremor [Kruskal-Wallis statistic = 9.874, $p = 0.0197$], which was significantly higher in EtOH-WDL (12 h) than CTRLs [$p = 0.0201$, Dunn's multiple comparisons test]; tail stiffness [Kruskal-Wallis statistic = 20.0, $p = 0.0002$], which was significantly higher in EtOH-WDL (12 h) [$p = 0.0025$, Dunn's multiple comparisons test] and EtOH-WDL (48 h) rats [$p = 0.0094$, Dunn's multiple comparisons test] than CTRL rats; and irritability to touch [Kruskal-Wallis statistic = 19.95, $p = 0.0002$], which was significantly higher in EtOH-WDL (12 h) than CTRLs [$p = 0.0001$, Dunn's multiple comparisons test].

The administration of L-DOPA in EtOH-WDL rats significantly decreased withdrawal global score [two-tailed Mann-Whitney test, including L-DOPA treatment as factor: EtOH-WDL (12 h) + L-DOPA vs. EtOH-WDL (12 h): $U= 5.0$, $p = 0.0040$] and irritability to touch [two-tailed Mann-Whitney test EtOH-WDL (12 h) + L-DOPA vs. EtOH-WDL (12 h): $U= 9.0$, $p = 0.0131$] when compared to vehicle.

Aversive limbic memory

We explored the consequences of the abrupt abstinence from alcohol chronic exposure on learning and memory processes that occur when rats adapt their behavior on the basis of the association with an aversive experience.

To address this issue, we used a novel task that enables to study the formation of limbic memory as a result of the acquisition and retrieval of fear-conditioning-biased declarative memory traces by assessing rat discrimination of an “emotional-object” and object-place

aversion (Brancato et al., 2016) (Fig. 1a). We found that whereas control- and chronically-EtOH exposed rats avoided the exploration of the fear-conditioned cue and displayed conditioned object-place aversion, early withdrawn rats from a chronic alcohol diet (EtOH-WDL) displayed disrupted acquisition of cue-paired aversive inputs such as decreased emotional object avoidance [one-way ANOVA, including treatment as main factor: $F_{(2, 21)} = 10.51$, $p = 0.0007$; Bonferroni post hoc test: CTRL vs EtOH-WDL $t = 4.516$, $df = 21$, $p < 0.001$; EtOH-CHR vs. EtOH-WDL $t = 2.945$, $df = 21$, $p < 0.05$] (Fig. 1b) and decreased target zone aversion [1-way Anova: $F_{(2, 21)} = 27.51$, $p < 0.0001$; Bonferroni post hoc test: CTRL vs EtOH-WDL $t = 6.542$, $df = 21$, $p < 0.001$; EtOH-CHR vs. EtOH-WDL $t = 6.299$, $df = 21$, $p < 0.001$] (Fig. 1c) with respect to alcohol-naïve control (CTRL) and chronically-EtOH-exposed (EtOH-CHR) rats, notwithstanding the absence of sensory/motor impairment in terms of total distance travelled (TDT) when video-tracked during the BSL epoch in context A chamber [Kruskal-Wallis test, $p = 0.2685$] (Fig. 1d), and tail flick latency following the EOR test [1-way ANOVA, $F_{(2, 21)} = 0.2070$, $p = 0.8147$] (Fig. 1e).

When L-Dopa (6 mg/kg, s.c., in association with benserazide 6 mg/kg, s.c) was administered 1 h before the fear conditioning paradigm at 12 h of abstinence, rats reversed their behavioral pattern and displayed acquisition and retrieval of the cue-fear association in a similar pattern as alcohol-naïve controls. Indeed, EtOH-WDL+L-DOPA treated rats displayed increased emotional object avoidance [two-way ANOVA, including withdrawal and L-DOPA treatment as factors, L-DOPA: $F_{(1, 28)} = 19.96$, $p = 0.0001$; withdrawal: $F_{(1, 28)} = 10.97$, $p = 0.0026$; interaction: $F_{(1, 28)} = 13.50$, $p = 0.0010$; Bonferroni post hoc test: CTRL + vehicle vs. EtOH-WDL + vehicle $t = 4.94$, $df = 28$, $p = 0.0002$; EtOH-WDL + vehicle vs. EtOH-WDL+L-DOPA $t = 5.757$, $df = 28$, $p < 0.001$] (Fig. 2a) and target zone aversion score [two-way ANOVA considering withdrawal and L-DOPA treatment as factors, L-DOPA: $F_{(1, 28)} = 21.09$, $p < 0.0001$; withdrawal: $F_{(1, 28)} = 82.68$, $p < 0.0001$; Bonferroni post hoc test: CTRL+vehicle vs. EtOH-WDL+vehicle $t = 7.068$, $df = 28$, $p <$

0.0001; EtOH-WDL + vehicle vs. EtOH-WDL+L-DOPA t = 3.886, df = 28, p = 0.0034] (Fig. 2b) up to CTRL level.

Interestingly, limbic memory disruption in EtOH-WDL rats was recorded in the EOR task after 48h and 14 days of withdrawal, highlighting the rigid persistence of the disrupted processing of emotionally salient information. Indeed, at 48 h and 14 days of withdrawal, EtOH-WDL rats showed decreased emotional object avoidance [two-way ANOVA, including withdrawal and L-DOPA treatment as factors, L-DOPA: $F_{(1, 42)}$ = 7.188, p = 0.0104; withdrawal: $F_{(2, 42)}$ = 14.52, p < 0.0001; interaction: $F_{(2, 42)}$ = 0.7173, p = 0.4940; Bonferroni post hoc test: CTRL+vehicle vs. EtOH-WDL(48 h)+vehicle t = 4.129, df = 42, p = 0.0025; CTRL+vehicle vs. EtOH-WDL(14 d)+vehicle t = 3.755, df = 42, p = 0.0079] (Fig. 2c) and target zone aversion score [two-way ANOVA including withdrawal and L-DOPA treatment as factors, L-DOPA: $F_{(1, 42)}$ = 3.6, p = 0.0647; withdrawal: $F_{(2, 42)}$ = 30.62, p < 0.0001; interaction: $F_{(2, 42)}$ = 1.106, p = 0.3402; Bonferroni post hoc test: CTRL+vehicle vs. EtOH-WDL(48 h)+vehicle t = 4.19, df = 42, p = 0.0021; CTRL+vehicle vs. EtOH-WDL(14 d)+vehicle t = 3.472, df = 42, p = 0.0181] (Fig. 2d), with respect to alcohol-naïve controls (CTRL). L-DOPA administration did not exert the same rescuing effect on aversive limbic memory when it was administered at 48 h and 14 d of withdrawal [emotional-object avoidance, Bonferroni post hoc: EtOH-WDL(48 h)+vehicle vs. EtOH-WDL(48 h)+L-DOPA t = 1.725, df = 42, p > 0.999; EtOH-WDL(14 d)+vehicle vs. EtOH-WDL(14 d)+L-DOPA t = 2.292, df = 42, p = 0.4044] (Fig. 3a); target-zone aversion score, Bonferroni post hoc: EtOH-WDL(48 h)+vehicle vs. EtOH-WDL(48 h)+L-DOPA t = 0.3578, df = 42, p > 0.999; EtOH-WDL(14 d)+vehicle vs. EtOH-WDL(14 d)+L-DOPA t = 0.6285, df = 42, p > 0.999] (Fig. 2c-d).

In contrast, the rescuing effect of early (12 h withdrawal) L-DOPA administration was dose-dependent on both emotional object avoidance [one-way ANOVA, considering treatment as main factor: $F_{(2, 21)}$ = 9.275, p = 0.0013; Bonferroni post hoc test: EtOH-

WDL+vehicle vs. EtOH-WDL +L-DOPA 6.0 mg/kg t = 4.277, df = 21, p < 0.01] (Fig. 2e) and target zone aversion score [one-way ANOVA considering treatment as main factor: $F_{(2, 21)}$ = 7.34, p = 0.0038; Bonferroni post hoc test: EtOH-WDL+vehicle vs. EtOH-WDL +L-DOPA 6.0 mg/kg t = 3.386, df = 21, p < 0.01; EtOH-WDL+L-DOPA 1.5 mg/kg vs. EtOH-WDL +L-DOPA 6.0 mg/kg t = 3.246, df = 21, p < 0.05] (Fig. 2f). The dose of 1.5 mg/kg was discarded for further testing.

Structural architecture of MSN dendritic spines

Data of confocal microscopy on Golgi-Cox stained MSNs of the NAc shell (Fig. 3a-e) highlighted that early EtOH withdrawal produced a selective and significant reduction (-49.89 ± 5.15 vs CTRL) in the density of long-thin spines compared to CTRL rats [two-way ANOVA including withdrawal and L-DOPA treatment as factors: effect of withdrawal $F_{(1, 23)}$= 12.7, p = 0.0016; Bonferroni post hoc test t = 5.637, df = 23, p < 0.001, Fig. 3b-c]. Subsequent immunostaining for both tyrosine hydroxylase (TH) and post-synaptic density protein (PSD-95) measured in NAc shell slices from 12-h withdrawn rats, revealed a significant reduction in the immunoreactivity for both TH [44.34 ± 3.2 %; two-way ANOVA including withdrawal and L-DOPA treatment as factors: effect of withdrawal $F_{(1, 23)}$ = 171.1, p < 0.001; Bonferroni post hoc test t = 10.18, df = 23, p < 0.001] and PSD-95 [59.75 ± 4.3 %; two-way ANOVA including withdrawal and L-DOPA treatment as factors: effect of withdrawal $F_{(1, 23)}$= 4.43, p=0.0464; Bonferroni post hoc test t = 4.671, df = 23, p < 0.001] relative to CTRL rats (Fig. 3d, e).

We then evaluated whether restoring DA signaling during withdrawal might also retrieve the disarranged architecture of the MSN synaptic triad in the NAc shell. Notably, the acute treatment with the DA precursor L-DOPA (6 mg/kg s.c. plus benserazide 6 mg/kg s.c) within the first 12h abstinence and 1h prior to rats sacrifice, proved efficacy in: selectively expanding the density of long-thin spines to similar values as controls [two-way ANOVA

including withdrawal and L-DOPA treatment as factors: effect of L-DOPA $F_{(1, 23)} = 11.28$, $p = 0.0027$; Bonferroni post hoc test $t = 5.906$, $df = 23$, $p < 0.001$], restoring the immunolabeling for PSD-95 in the NAc [two-way ANOVA including withdrawal and L-DOPA treatment as factors: effect of L-DOPA $F_{(1, 23)} = 26.66$, $p < 0.001$; Bonferroni post hoc test $t = 7.313$, $df = 23$, $p < 0.001$] and increasing TH levels in DA efferent projections [two-way ANOVA including withdrawal and L-DOPA treatment as factors: effect of L-DOPA $F_{(1, 23)} = 6.034$, $p=0.022$; Bonferroni post hoc test $t = 2.99$, $df = 23$, $p < 0.05$] (Fig. 3 b-e).

Long-term synaptic plasticity

Our functional analysis has confirmed previous evidence showing that, in association with changes in dendritic spine density, TH immunoreactivity and postsynaptic PSD 95 expression, alcohol withdrawal dramatically and selectively decreases the formation of LTD (Spiga et al 2014). In particular, in single voltage-clamped MSNs of the NAc shell, NMDAR-dependent LTD, induced by low-frequency stimulation (LFS, 500 stimuli at 1 Hz) paired with membrane depolarization (-50 mV), was almost completely abolished when tested 12 h after termination of EtOH exposure (Fig. 4a-d). We here extend this finding by showing that the loss of LTD formation was long-lasting as it was still apparent when tested after 48 h and up to 14 days of withdrawal [$F_{(3,31)} = 10.05$; $p = 0.0001$; Bonferroni's post-hoc test, CTRL vs EtOH-WDL (12 h) $p = 0.0005$, CTRL vs EtOH-WDL (48 h) $p = 0.0004$, CTRL vs EtOH-WDL (14 d) $p = 0.0006$] (Fig. 4 a-d). In a more detailed evaluation of data obtained in EtOH-WDL (12h) compared to CTRL group, the scatter graph in Fig. 4d shows that the abolishment of LTD is present in roughly half of the cells tested (6 of 11 tested) (Fig. 4d).

Glutamatergic excitatory neurotransmission in MSNs of the NAc shell is heavily controlled by DAergic afferents coming from the VTA (Russo and Nestler, 2013). Because the immunolabelling of TH is markedly reduced in EtOH-WDL rats (present data and Spiga et

al., 2014), consistent with the idea of a “hypodopaminergic state” associated with EtOH withdrawal (**Melis et al., 2005**), we tested the capability of the in vivo L-DOPA treatment of EtOH-dependent rats, in restoring the hampered long-term plasticity observed at glutamatergic synapses. L-DOPA (6 mg/kg, s.c.) and benserazide (6 mg/kg, s.c.) treatment, administered 1 h before the sacrifice of EtOH-WDL rats, restored LTD formation (50 ± 4.0% of baseline) to a value similar to that found in CTRL animals [$F_{(2,30)}$ = 11.58, p = 0.0002; Bonferroni’s post-hoc test, CTRL vs EtOH-WDL 0.0002, EtOH-WDL VS EtOH-WDL+L-DOPA 0.0084] (Fig. 5 a-c), but failed to modify LTD formation in either CTRL and EtOH-CHR rats (Fig. 5 g-h). To further explore the effects of increasing DAergic signaling in the NAc of EtOH withdrawn rats, in a different set of experiments brain slices containing the NAc shell, obtained from animals of the different experimental groups, were bath-perfused with 10 μM DA (Lavin and Grace, 2001) for 5 min prior to the application of LFS. DA perfusion completely rescued LTD formation (46 ± 4% of baseline) in slices obtained from EtOH-WDL animals (Fig. 5 d-f) [$F_{(2,33)}$ = 11.45, p = 0.0002; Bonferroni’s post-hoc test, CTRL vs EtOH-WDL p = 0.0016, EtOH-WDL VS EtOH-WDL+DA p = 0.0019, CTRL vs EtOH-WDL+DA p = 0.999], but did not alter significantly the extent of LTD in slices from either CTRL and EtOH-CHR rats (Fig. 5 g-h).

A recent study by Yagishita et al., 2014, reported that synaptically released DA was able to empower Hebbian plasticity of D1-positive MSNs in the NAc core by an enlargement of dendritic spine heads within 1 s, and a decay of few seconds. Taking advantage of such findings, in order to evaluate whether WDL-induced effect may be related to a specific sensitivity of D1 or D2 containing neurons in the NAc shell, we bath-applied DA (10 μM) in the presence of the D1 and D2 receptor antagonists SCH23390 and sulpiride, respectively. Fig. 6 shows that co-perfusion of SCH23390, but not sulpiride, fully prevented the capacity of DA to restore LTD formation in EtOH-WDL rats [$F_{(4,45)}$ = 8.86, p

543 = 0.0001; Bonferroni's post-hoc test, EtOH-WDL vs EtOH-WDL + DA p = 0.0049, EtOH-
544 WDL vs EtOH-WDL + DA + SCH p = 0.8446, EtOH-WDL vs EtOH-WDL + DA + Sulpiride p
545 = 0.0049], indicating that D1 receptors are selectively involved in the restoring effect of DA
546 on LTD formation in EtOH-WDL (12 h) rats. **T**he scatter graph in Fig. 6c shows that the
547 different distribution of WDL-induced impairment in LTD formation is still apparent in the
548 presence of D1 antagonist SCH but not with D2 antagonist sulpiride, where all cell tested
549 showed a consistent LTD formation. In addition, both in vivo L-DOPA treatment and bath-
550 perfusion of NAc slices with DA reversed the reduction in NMDAR/AMPAR ratio in EtOH-
551 WDL rats (Spiga et al., 2014) to a value similar to CTRL animals [$F_{(3,317)} = 14.56$, p =
552 0.0001; Bonferroni's post-hoc test, CTRL vs EtOH-WDL p = 0.0001, EtOH-WDL VS EtOH-
553 WDL+L-DOPA p = 0.0001, EtOH-WDL VS EtOH-WDL+DA p = 0.0001] (Fig. 7).
554
555 **In vivo microdialysis studies**
556 Our neurochemical analysis confirmed previous evidence indicating that EtOH
557 withdrawal is associated with a marked reduction in DA levels (Diana et al., 1993). Indeed,
558 basal DA extracellular levels in the NAc shell of EtOH-WDL and CTRL rats, assessed by in
559 vivo microdialysis, were respectively 48.9 ± 4 and 99.36 ± 7 (mean ± SEM; N = 4),
560 expressed as fmoles/20 ul sample. In particular, the RM two-way ANOVA on basal DA
561 levels, including ethanol withdrawal as the between-subject factor and time as the
562 repeated measure factor, showed a significant main effect of ethanol withdrawal [$F_{(1, 6)}$ =
563 44.54, p = 0.0005] with no effects of time [$F_{(2, 12)} = 1.192$, p = 0.3371] or their interaction [F
564 $_{(2, 12)} = 0.7624$, p = 0.4879] (Fig. 8a).
565 In order to study the effects of L-DOPA on the hypodopaminergic state of the NAc in
566 ethanol withdrawal, the time course of extracellular DA levels in NAc shell of EtOH-WDRL
567 (12 h) and CTRL rats following L-DOPA/benserazide administration (6/6 mg/kg s. c.) was
568 monitored. As shown in Fig 8a L-DOPA/benserazide administration increased extracellular

DA level in EtOH-WDL rats, up to CTRL's levels. In more detail, the RM two-way ANOVA on DA levels following the L-DOPA/benserazide administration, including ethanol withdrawal as the between-subject factor and time as the repeated measure factor, showed a significant main effect of ethanol withdrawal [$F_{(1, 6)} = 6.207$, $p = 0.0471$] and time [$F_{(9, 54)} = 2.410$, $p = 0.0223$] but not of their interaction [$F_{(9, 54)} = 1.426$, $p = 0.2003$]. When Sidak's multiple comparisons test was considered, it indicated that EtOH-WDL group differed from CTRL only at the time point 0, when the L-DOPA administration occurred [$t = 3.234$, $p < 0.05$, $df = 60$] (Fig. 8a).

Notably, when DA levels were expressed as % of baseline, RM two-way ANOVA on DA levels following L-DOPA administration showed a main effect of group [$F_{(1,6)} = 13.41$; $p < 0.05$], and time [$F_{(9,54)} = 3.15$; $p < 0.05$], and a significant group x time interaction [$F_{(9,54)} = 3.25$; $p < 0.05$]. Tukey's post hoc tests showed a larger increase of dialysate DA in the NAc shell of EtOh-WDRL (12 h) as compared to basal (filled symbols, $t = 5.564$, $p < 0.001$, $df = 54$; $t = 4.490$, $p < 0.001$, $df = 54$) and to dialysate DA in the NAc shell of CTRL rats [40 min: $t = 4.837$, $p < 0.001$, $df = 60$; 60 min: $t = 3.984$, $p < 0.01$, $df = 60$] (Fig. 8b).

Discussion

This research took advantage of a multidisciplinary approach aimed at visualize, in alcohol-dependent rats, the structural, functional and behavioral outcomes of alcohol withdrawal as a tridimensional *unicum*, a whole (mal)adaptive process, which recognizes in the hypodopaminergic state a causal mechanistic basis. The principal finding consists in the recovery of alcohol withdrawal-associated abnormal limbic memory and synaptic plasticity, by strengthening DA transmission with acute L-DOPA administration.

Aberrant aversive limbic memory

595 Alcohol-related impairment of aversive memories could positively bias a drinker's
596 memory of past negative drinking episodes, and this, in turn, may increase the likelihood of
597 future alcohol consumption. Thus, it was our first requirement to determine in alcohol-
598 dependent rats how withdrawal affects aversive limbic memory, a complex function that
599 integrates the consciously accessible explicit- and the unconscious implicit memory. Our
600 evidence suggests that experience-dependent plasticity in the NAc during alcohol
601 withdrawal is associated to defects in neural circuitries that normally serve fear-related
602 learning. Indeed whereas control- and chronically alcohol exposed- rats avoided the fear-
603 conditioned cue and displayed conditioned object-place aversion in the EOR test, alcohol-
604 withdrawn rats displayed a disrupted processing of emotionally salient information,
605 notwithstanding the absence of sensory/motor impairment.
606 Impairment in learning, memory and recognition are reported in humans during alcohol
607 withdrawal (Parsons and Nixon, 1993; Smith and Atkinson, 1995); alcoholic patients and
608 binge drinkers (Stephens and Duka, 2008) display reduced galvanic skin responses to a
609 fear conditioned tone (Stephens et al., 2005) and, when presented with fearful facial
610 expressions, show inaccurate fear recognition (Townshend and Duka, 2003).
611 In agreement with the human data, alcohol withdrawal severely disrupts fear conditioning
612 in mice in a Pavlovian paradigm (Kitaichi et al., 1995). In the laboratory setting, Pavlovian
613 fear conditioning represents the quintessential method of investigating implicit emotional
614 learning (LeDoux, 1996). Nevertheless, it is accompanied by some limitations including
615 (Antoniadis and McDonald, 1999): the assessment of single responses of fear as a
616 measure of implicit memory; the use of non-discriminative paradigms; the association
617 between the unconditioned stimulus and the environmental context. Rather, the evaluation
618 of limbic memory by the EOR test overcomes these limitations since it implies the
619 recruitment of cognitive networks designed to the encoding and storage of explicit memory
620 representation (object-recognition), and their integration with the emotional valence of the

fear-conditioning, in an unconditioned context. Indeed, memories for emotional situations are not only formed implicitly, as the explicit memory circuits can process their own memories of emotional situations. Notably, dysfunctional aversive limbic memory was still observed after 48h and 14 days of abstinence, highlighting the persistence of defects in the neural circuitries that normally serve fear-related learning.

Aberrant architectural and functional structure of NAc MSNs

DA plays a crucial role in the morphological integrity of dendritic spines in MSNs in the NAc (Freund et al., 1984). Decreased DA levels or loss of DA neurons, such as in Parkinson's disease models, reduce the number of dendritic spines (Ingham et al., 1993; Solis et al., 2007; Garcia et al., 2010), whereas increase in DA levels, by cocaine and amphetamine, enhances the number of dendritic spines in MSNs (Robinson and Kolb, 1997, 1999; Li et al., 2003; Lee et al., 2006; Singer et al., 2009). In this study, withdrawal from alcohol consumption induced signs of aberrant plasticity in the NAc, evidenced by the simultaneous visualization of decreased TH and PSD-95 levels, and disarrangement in dendritic spine architecture. The selective loss of thin spines is suggestive of a model in which changes in spine volume and density regulate the anatomy and activity of the mesocorticolimbic network (Matsuzaki et al., 2004; Nusser et al., 1998; Kharazia and Weinberg, 1999; Okamoto et al., 2004). Our functional analysis has indeed provided evidence that, in association with changes in dendritic spine density and synaptic protein expression, alcohol withdrawal virtually abolished NMDAR-dependent LTD as indexed by patch clamp recordings; moreover, a significant decrease in NMDAR/AMPAR ratio compared to CTRL and EtOH-CHR animals was also observed, likely as a consequence of the marked reduction in NMDAR function. The impaired NMDA-dependent plasticity associated with alcohol withdrawal is consistent with the decreased immunoreactivity for PSD-95 that plays a crucial role as an anchoring protein for NMDA receptors in the spine

membrane (Zhang et al., 2009). Notably, the impairment in LTD paralleled the time course of limbic memory impairment, and persisted until day 14 of withdrawal.

Altogether, these data indicate that in NAc MSNs, alcohol withdrawal-induced DAergic blunting - witnessed by reduced TH expression - impairs NMDAR signaling through the reduced expression of PSD-95 and associated long thin spine loss. This effect in turn may lead to dampening of LTD formation in these synapses and result in dysfunctional aversive limbic memory.

Boosting dopamine transmission

The aberrant synaptic plasticity observed in the aforementioned conditions might be the cellular background at the core of the inability to correctly process aversive environmental stimuli into salient memory engrams in alcohol-withdrawn rats. This potentially suggests that counteracting the morphological abnormalities recorded in the striatal triad by boosting DA tone during alcohol withdrawal, would shape functional Hebbian plasticity and restore limbic memory. This hypothesis was challenged by injecting withdrawn rats with L-DOPA/benserazide, 1 h prior to animals' sacrifice, and recording DA release by in vivo microdialysis in the NAc shell. As expected, the down-regulated DA release in EtOH-WDL was raised to control rats' values by L-DOPA treatment, with almost 300% increase from basal levels. Interestingly, DA uprise proved effective in selectively expanding the density of long-thin spines to similar values as controls and produced a reinstatement of the immunolabeling for TH and PSD-95. Notably, the rapid effect of L-DOPA on morphology and PSD-95 immunohistology observed in the present study is consistent with evidence showing that spinogenesis involves fast dynamics (Bresler et al., 2001; Kozorovitskiy et al., 2015). Dopamine stimulation is associated with the recruitment of PSD95 to the postsynaptic density from a diffuse dendritic cytoplasmic pool within 20–60 min (Fasano et al., 2013; Bresler et al., 2001). PSD-95 recruited to the synaptic sites

673 complex with NMDA receptors, increase their signaling thus promoting correct set up of
674 synaptic plasticity mechanisms (Wyneken et al., 2004). In this context, they may serve as
675 key determinants in the machinery underlying the interplay between glutamate and
676 dopamine pathways in the striatum (De Bartolomeis and Tomasetti, 2012; Colledge et al.,
677 2000; Swayze et al., 2004). Indeed, the increase in DA availability was also associated to
678 the recovery of withdrawal-related hampered long-term plasticity of the glutamatergic
679 synapse in the triad, with LTD reaching similar values as controls. Further, LTD formation
680 was also rescued in brain slices, obtained from EtOH-WDL animals, in the presence of 10
681 μM DA applied for just 5 min prior to the induction of LTD. Accordingly, both in vivo L-
682 DOPA treatment and DA bath-perfusion of NAc slices reversed the reduction in
683 NMDAR/AMPAR ratio in EtOH-WDL rats to control levels.
684 While synaptic plasticity is observed in both D1- and D2-MSNs (Shen et al., 2008),
685 alcohol-induced plasticity is predominantly observed in striatal D1-MSNs, where alcohol
686 consumption affects NMDAR activity (Cheng et al., 2017). Consistently, our data confirm
687 that LTD formation was virtually observed in all the MSNs of CTRL group (Fig 4d).
688 However in EtOH-WDL rats LTD was apparent in about 40% of cells tested, suggesting
689 two different populations of cells affected by WDL. The fact that SCH23390, but not
690 sulpiride, completely prevented the capability of DA to restore LTD formation in EtOH-WDL
691 rats, may suggest that MSNs expressing D1are those selectively involved in the aberrant
692 plasticity associated with EtOH-WDL as well as in the restoring effect of DA, strengthening
693 the idea that D1-MSN LTD recovery might be a potential therapeutic strategy for alcohol
694 use (Ma et al., 2018). Overall we suggest that restoring DA levels in the NAc during early
695 alcohol withdrawal re-establishes D1-signaling in the MSN synaptic triad thus normalizing,
696 likely via intra-spinous calcium levels (Segal and Andersen, 2000), spine morphology and
697 integrative properties, and revitalizing Hebbian learning. Indeed, DA signaling in the NAc is
698 of exceptional importance for gating attention and facilitating conditioned stimulus

699 associations during fear-conditioning (Bromberg-Martin et al., 2010; Pezze and Feldon,
700 2004; Wise, 2004). Hence, we assumed that restoring blunted DA signaling and altered
701 connectivity in the NAc before the acquisition phase of the limbic memory task would
702 rescue the impairment in aversive limbic memory here reported. Accordingly, we injected
703 withdrawn rats with L-DOPA/benserazide 1h before the fear-conditioning paradigm at 12h
704 abstinence: in addition to the significant reduction in withdrawal symptoms, EtOH-WDL
705 rats displayed acquisition and retrieval of the cue-fear association displaying emotional
706 object-recognition and target zone avoidance, similar to controls. However, L-DOPA effect
707 was limited to early stages of withdrawal since when injected at 48h and 14 day of
708 abstinence it was ineffective, suggesting that DA replacement can rescue the withdrawn
709 maladaptive synapses just in the early “fluid” and responsive state. Overall this evidence
710 highlights a functional correlation between neuronal and behavioral learning mechanisms
711 in the NAc that, besides encoding rewarding experiences, cooperates, as a crucial hub, to
712 the integration of the multiple circuitries that contribute to the formation of limbic memory
713 (Ramirez et al., 2015).
714
715 ***Conclusions***
716 Alcohol-related impairment in aversive memory of events that occur in the
717 nonlaboratory setting could lower the possibility that negative alcohol-related outcomes
718 discourage future consumption; this might explain the disregard of negative drinking-
719 related consequences observed in alcohol-dependent individuals.
720 Overall our data suggest that strengthening DA signal, during early withdrawal, may
721 restore the structural architecture of the NAc MSNs triad, pre and postsynaptic indices of
722 functional plasticity that allow those synapses to encode emotionally relevant information
723 and rescue flexibility to the neuronal circuits that process limbic memory formation. Under
724 these conditions, drugs- or non- pharmacological tools such as transcranial magnetic

725 stimulation (Diana et al., 2017)- capable of boosting Da signaling (Steensland et al., 2012)
726 during the onset of the withdrawal maladaptive process, could help in breaking the
727 addictive cycle and prove useful in the treatment of alcohol addiction.

728 **List of References**

729 Antoniadis EA, McDonald RJ (1999) Discriminative fear conditioning to context expressed
730 by multiple measures of fear in the rat. Behav Brain Res. 101(1):1-13.
731
732 Berry KP, Nedivi E (2017) Spine Dynamics: Are They All the Same? Neuron 96(1):43-55
733
734 Bosch M, Castro J, Saneyoshi T, Matsuno H, Sur M, Hayashi Y (2014) Structural and
735 molecular remodeling of dendritic spine substructures during long-term potentiation.
736 Neuron 82(2):444-59.
737
738 Bourne J, Harris KM (2007) Do thin spines learn to be mushroom spines that remember?
739 Curr Opin Neurobiol. 17(3):381-6.
740
741 Brancato A, Lavanco G, Cavallaro A, Plescia F, Cannizzaro C (2016) The use of the
742 Emotional-Object Recognition as an assay to assess learning and memory associated to
743 an aversive stimulus in rodents. J Neurosci Methods 274:106-115.
744
745 Bresler T, Ramati Y, Zamorano PL, Zhai R, Garner CC, Ziv NE (2001) The dynamics of
746 SAP90/PSD-95 recruitment to new synaptic junctions. Mol Cell Neurosci. 18(2):149-67
747
748 Bromberg-Martin ES, Matsumoto M, Hikosaka O (2010) Dopamine in motivational control:
749 rewarding, aversive, and alerting. Neuron. 68(5):815-34.
750
751 Carr DB, Sesack SR (1996) Hippocampal afferents to the rat prefrontal cortex: synaptic
752 targets and relation to dopamine terminals. J Comp Neurol 369(1):1-15.
753

754 Cheng Y, Huang CCY, Ma T, Wei X, Wang X, Lu J, Wang J (2017) Distinct Synaptic
755 Strengthening of the Striatal Direct and Indirect Pathways Drives Alcohol Consumption.
756 Biol Psychiatry 81(11):918-929.
757
758 Colledge M, Dean RA, Scott GK, Langeberg LK, Huganir RL, Scott JD (2000) Targeting of
759 PKA to glutamate receptors through a MAGUK-AKAP complex. Neuron. 27(1):107-19.
760
761 Darvas M, Fadok JP, Palmiter RD (2011) Requirement of dopamine signaling in the
762 amygdala and striatum for learning and maintenance of a conditioned avoidance
763 response. Learn Mem. 18(3):136-43
764
765 De Bartolomeis A, Tomasetti C (2012) Calcium-dependent networks in dopamine-
766 glutamate interaction: the role of postsynaptic scaffolding proteins. Mol Neurobiol.
767 46(2):275-96.
768
769 Diana M, Pistis M, Carboni S, Gessa GL, Rossetti ZL (1993) Profound decrement of
770 mesolimbic dopaminergic neuronal activity during ethanol withdrawal syndrome in rats:
771 electrophysiological and biochemical evidence. Proc Natl Acad Sci U S A. 90(17):7966-9.
772
773 Diana M, Raij T, Melis M, Nummenmaa A, Leggio L, Bonci A (2017) Rehabilitating the
774 addicted brain with transcranial magnetic stimulation. Nat Rev Neurosci. 18(11):685-693.
775
776 Fasano C, Bourque MJ, Lapointe G, Leo D, Thibault D, Haber M, Kortleven C,
777 Desgroseillers L, Murai KK, Trudeau LÉ (2013) Dopamine facilitates dendritic spine
778 formation by cultured striatal medium spiny neurons through both D1 and D2 dopamine
779 receptors. Neuropharmacology. 67:432-43.

780

781 Freund TF, Powell JF, Smith AD (1984) Tyrosine hydroxylase-immunoreactive boutons in
782 synaptic contact with identified striatonigral neurons, with particular reference to dendritic
783 spines. Neuroscience 13(4):1189-215.

784

785 Garcia BG, Neely MD, Deutch AY (2010) Cortical regulation of striatal medium spiny
786 neuron dendritic remodeling in parkinsonism: modulation of glutamate release reverses
787 dopamine depletion-induced dendritic spine loss. Cereb Cortex. 20(10):2423-32.

788

789 Gass JT, Olive MF (2008) Glutamatergic substrates of drug addiction and alcoholism.
790 Biochem Pharmacol. 75:218–265.

791

792 Heilig M, Egli M, Crabbe JC, Becker HC (2010) Acute withdrawal, protracted abstinence
793 and negative affect in alcoholism: are they linked? Addict Biol. 15(2):169-84.

794

795 Hyman SE, Malenka RC, Nestler EJ (2006) Neural mechanisms of addiction: the role of
796 reward-related learning and memory. Annu Rev Neurosci. 29:565-98.

797

798 Ingham CA, Hood SH, van Maldegem B, Weenink A, Arbuthnott GW (1993) Morphological
799 changes in the rat neostriatum after unilateral 6-hydroxydopamine injections into the
800 nigrostriatal pathway. Exp Brain Res. 93(1):17-27.

801

802 Kalivas PW, Volkow ND (2011) New medications for drug addiction hiding in glutamatergic
803 neuroplasticity. Mol Psychiatry 16:974–986.

804

805 Kasai H, Fukuda M, Watanabe S, Hayashi-Takagi A, Noguchi J (2010) Structural

dynamics of dendritic spines in memory and cognition. Trends Neurosci. 33(3):121-9.

Kauer JA, Malenka RC (2007) Synaptic plasticity and addiction. Nat Rev Neurosci. 8:844–858.

Kharazia VN, Weinberg RJ (1999) Immunogold localization of AMPA and NMDA receptors in somatic sensory cortex of albino rat. J Comp Neurol. 412(2):292–302

Kiefer F, Dinter C (2013) New approaches to addiction treatment based on learning and memory. Curr Top Behav Neurosci. 13:671-84.

Kitaichi K, Minami Y, Amano M, Yamada K, Hasegawa T, Nabeshima T (1995) The attenuation of suppression of motility by triazolam in the conditioned fear stress task is exacerbated by ethanol in mice. Life Sci. 57(8):743-53.

Koob GF, Le Moal M (2001) Drug addiction, dysregulation of reward, and allostasis. Neuropsychopharmacology 24(2):97-129.

Koob GF, Volkow ND (2010) Neurocircuitry of addiction. Neuropsychopharmacology. 35(1):217-38.

Kozorovitskiy Y, Peixoto R, Wang W, Saunders A, Sabatini BL (2015) Neuromodulation of excitatory synaptogenesis in striatal development. Elife. 9;4. pii: e10111.

Lavine A and Grace AA (2001) Stimunlation of D1-type dopamine receptors enhances excitability in prefrontal cortical pyramidal neurons in a state-dependent manner.

832 Neuroscience. 104(2):335-46

833

834 LeDoux J (1996) Emotional networks and motor control: a fearful view. Prog Brain Res.
835 107:437-46.

836

837 Lee KW, Kim Y, Kim AM, Helmin K, Nairn AC, Greengard P (2006) Cocaine-induced
838 dendritic spine formation in D1 and D2 dopamine receptor-containing medium spiny
839 neurons in nucleus accumbens. Proc Natl Acad Sci U S A. 103(9):3399-404.

840

841 Lendvai B, Stern EA, Chen B, Svoboda K (2000) Experience-dependent plasticity of
842 dendritic spines in the developing rat barrel cortex in vivo. Nature 404(6780):876-81.

843

844 Li Y, Kolb B, Robinson TE (2003) The location of persistent amphetamine-induced
845 changes in the density of dendritic spines on medium spiny neurons in the nucleus
846 accumbens and caudate-putamen. Neuropsychopharmacology. 28(6):1082-5

847

848 Ma T, Cheng Y, Roltsch Hellard E, Wang X, Lu J, Gao X, Huang CCY, Wei XY, Ji JY,
849 Wang J (2018) Bidirectional and long-lasting control of alcohol-seeking behavior by
850 corticostriatal LTP and LTD. Nat Neurosci. 21(3):373-383.

851

852 Matsuzaki M, Honkura N, Ellis-Davies GC, Kasai H (2004) Structural basis of long-term
853 potentiation in single dendritic spines. Nature 429(6993):761–766

854

855 **Melis M, Spiga S, Diana M (2005) The dopamine hypothesis of drug addiction:**
856 **hypodopaminergic state. Int Rev Neurobiol 63:101-154.**

857

858 Nestler EJ (2013) Cellular basis of memory for addiction. Dialogues Clin Neurosci.
859 15(4):431-43.
860
861 Nikolaus S, Beu M, de Souza Silva MA, Huston JP, Hautzel H, Mattern C, Antke C, Müller
862 HW (2016) Relationship between L-DOPA-induced reduction in motor and exploratory
863 activity and striatal dopamine D2 receptor binding in the rat. Front Behav Neurosci. 9:352.
864
865 Nusser Z, Lujan R, Laube G, Roberts JD, Molnar E, Somogyi P (1998) Cell type and
866 pathway dependence of synaptic AMPA receptor number and variability in the
867 hippocampus. Neuron 21(3):545-59.
868
869 Okamoto K, Nagai T, Miyawaki A, Hayashi Y (2004) Rapid and persistent modulation of
870 actin dynamics regulates postsynaptic reorganization underlying bidirectional plasticity.
871 Nat Neurosci. 7(10):1104–1112
872
873 Paxinos G, Watson C (1998). The Rat Brain in Stereotaxic Coordinates. 4th ed. London:
874 Academic Press.
875
876 Parsons OA, Nixon SJ (1993) Neurobehavioral sequelae of alcoholism. Neurol. Clin. 11:
877 205–218
878
879 Pezze MA, Feldon J (2004) Mesolimbic dopaminergic pathways in fear conditioning. Prog
880 Neurobiol. 74(5):301-20.
881
882 Pignatelli M, Umanah GKE, Ribeiro SP, Chen R, Karuppagounder SS, Yau HJ, Eacker S,
883 Dawson VL, Dawson TM, Bonci A (2017) Synaptic Plasticity onto Dopamine Neurons

884 Shapes Fear Learning. Neuron. 93(2):425-440.

885

886 Ramirez S, Liu X, MacDonald CJ, Moffa A, Zhou J, Redondo RL, Tonegawa S (2015)
887 Activating positive memory engrams suppresses depression-like behaviour. Nature.
888 522(7556):335-9.

889

890 Robinson TE, Kolb B (1999) Alterations in the morphology of dendrites and dendritic
891 spines in the nucleus accumbens and prefrontal cortex following repeated treatment with
892 amphetamine or cocaine. Eur J Neurosci.11(5):1598-604.

893

894 Robinson TE, Kolb B (1997) Persistent structural modifications in nucleus accumbens and
895 prefrontal cortex neurons produced by previous experience with amphetamine. J Neurosci.
896 17(21):8491-7.

897

898 Rothblat DS, Rubin E, Schneider JS (2001) Effects of chronic alcohol ingestion on the
899 mesostriatal dopamine system in the rat. Neurosci Lett. 300(2):63-6.

900

901 Russo SJ, Nestler EJ (2013) The brain reward circuitry in mood disorders. Nat Rev
902 Neurosci. 14(9):609-25.

903

904 Segal M, Andersen P (2000) Dendritic spines shaped by synaptic activity. Curr Opin
905 Neurobiol. 10(5):582–586.

906

907 Shen W, Flajolet M, Greengard P, Surmeier DJ (2008) Dichotomous dopaminergic control
908 of striatal synaptic plasticity. Science 321: 848–851

909

910 Singer BF, Tanabe LM, Gorny G, Jake-Matthews C, Li Y, Kolb B, Vezina P (2009)
911 Amphetamine-induced changes in dendritic morphology in rat forebrain correspond to
912 associative drug conditioning rather than nonassociative drug sensitization. Biol
913 Psychiatry. 65(10):835-40.
914
915 Smith DM, Atkinson RM (1995) Alcoholism and dementia. Int. J. Addict. 30:1843–1869
916
917 Solis O, Limón DI, Flores-Hernández J, Flores G (2007) Alterations in dendritic
918 morphology of the prefrontal cortical and striatum neurons in the unilateral 6-OHDA-rat
919 model of Parkinson's disease. Synapse 61(6):450-8.
920
921 Spiga S, Talani G, Mulas G, Licheri V, Fois GR, Muggironi G, Masala N, Cannizzaro C,
922 Biggio G, Sanna E, Diana M (2014) Hampered long-term depression and thin spine loss in
923 the nucleus accumbens of ethanol-dependent rats. Proc Natl Acad Sci U S A.
924 111(35):E3745-54.
925
926 Steensland P, Fredriksson I, Holst S, Feltmann K, Franck J, Schilström B, Carlsson A
927 (2012) The monoamine stabilizer (-)-OSU6162 attenuates voluntary ethanol intake and
928 ethanol-induced dopamine output in nucleus accumbens. Biol Psychiatry. 72(10):823-31.
929
930 Stephens DN, Duka T (2008) Cognitive and emotional consequences of binge drinking:
931 role of amygdala and prefrontal cortex. Philos Trans R Soc Lond B Biol Sci.
932 363(1507):3169-79.
933
934 Stephens DN, Ripley TL, Borlikova G, Schubert M, Albrecht D, Hogarth L, Duka T (2005)
935 Repeated ethanol exposure and withdrawal impairs human fear conditioning and

936 depresses long-term potentiation in rat amygdala and hippocampus. Biol Psychiatry.
937 58(5):392-400.
938
939 Swayze RD, Lisé MF, Levinson JN, Phillips A, El-Husseini A (2004) Modulation of
940 dopamine mediated phosphorylation of AMPA receptors by PSD-95 and AKAP79/150.
941 Neuropharmacology. 47(5):764-78.
942
943 Townshend JM, Duka T (2003) Mixed emotions: alcoholics' impairments in the recognition
944 of specific emotional facial expressions. Neuropsychologia 41(7):773-82.
945
946 Trachtenberg JT, Chen BE, Knott GW, Feng G, Sanes JR, Welker E, Svoboda K (2002)
947 Long-term in vivo imaging of experience-dependent synaptic plasticity in adult cortex.
948 Nature. 420(6917):788-94.
949
950 Uys JD, McGuier NS, Gass JT, Griffin WC 3rd, Ball LE, Mulholland PJ (2016) Chronic
951 intermittent ethanol exposure and withdrawal leads to adaptations in nucleus accumbens
952 core postsynaptic density proteome and dendritic spines. Addict Biol. 21(3):560-74.
953
954 Weiss F, Parsons LH, Schulteis G, Hyytiä P, Lorang MT, Bloom FE, Koob GF (1996)
955 Ethanol self-administration restores withdrawal-associated deficiencies in accumbal
956 dopamine and 5-hydroxytryptamine release in dependent rats. J Neurosci. 16(10):3474-
957 85.
958
959 Wise RA (2004) Dopamine, learning and motivation. Nat Rev Neurosci. 5(6):483-94.
960
961 Wyneken U, Marengo JJ, Orrego F (2004) Electrophysiology and plasticity in isolated

962 postsynaptic densities. Brain Res Brain Res Rev 47(1–3):54–70

963

964 Yagishita S, Hayashi-Takagi A, Ellis-Davies GC, Urakubo H, Ishii S, Kasai H. (2014). A
965 critical time window for dopamine actions on the structural plasticity of dendritic spines.
966 Science. 345(6204): 1616-1620.

967

968 Zhang J, Xu TX, Hallett PJ, Watanabe M, Grant SG, Isacson O, Yao WD (2009) PSD-95
969 uncouples dopamine-glutamate interaction in the D1/PSD-95/NMDA receptor complex. J
970 Neurosci. 29(9):2948-60.

971

972 Zhou FC, Anthony B, Dunn KW, Lindquist WB, Xu ZC, Deng P (2007) Chronic alcohol
973 drinking alters neuronal dendritic spines in the brain reward center nucleus accumbens.
974 Brain Research 1134:148–161

975

976 **Tables**

977 Table 1. Experimental design

Experiments		Groups	Analysis
Behavior	Signs of withdrawal	CTRL; EtOH-WDL; CTRL + L-DOPA; EtOH-WDL + L-DOPA	Kruskal-Wallis test - Dunn's post hoc test; factor: withdrawal Mann-Whitney U- test; factor: L-DOPA treatment
	Locomotor activity	CTRL; EtOH-CRH; EtOH-WDL	Kruskal-Wallis test; factor: treatment
	Emotional-object recognition test	CTRL; EtOH-CRH; EtOH-WDL; CTRL + L-DOPA; EtOH-WDL + L-DOPA	one-way ANOVA - Bonferroni post hoc test; factor: treatment; two-way ANOVA - Bonferroni post hoc test; factors: withdrawal; L-DOPA treatment
	Tail flick test	CTRL; EtOH-CRH; EtOH-WDL	one-way ANOVA; factor: treatment
Golgi Cox - Immunofluorescence	TH; PSD-95	CTRL; EtOH-WDL; CTRL + L-DOPA; EtOH-WDL + L-DOPA	two-way ANOVA - Bonferroni post hoc test; factors: withdrawal; L-DOPA treatment
	Spine analysis (stubby - mushroom - long thin -	CTRL; EtOH-WDL; CTRL + L-DOPA; EtOH-WDL + L-DOPA	two-way ANOVA - Bonferroni post hoc test; factors: withdrawal; L-DOPA treatment

	filopodia)		
Electrophysiology - AMPA/NMDA ratio; - LTD	in vivo - L-DOPA	CTRL; EtOH-CRH; EtOH-WDL CTRL + L-DOPA; EtOH-WDL + L-DOPA	one-way ANOVA - Bonferroni post hoc test; factor: treatment two-way ANOVA - Bonferroni post hoc test; factors: withdrawal; L-DOPA treatment
	in vitro - DA	CTRL; EtOH-WDL; EtOH-WDL+DA; EtOH-WDL+DA+SCH; EtOH-WDL+DA+Sulp	one-way ANOVA - Bonferroni post hoc; factor: treatment
Microdialysis	in vivo	CTRL; EtOH-WDL CTRL + L-DOPA; EtOH-WDL + L-DOPA	two-way ANOVA - Sidak/Tuckey post hoc test; factors: withdrawal; time

Table 2. Rating of behavioral signs of withdrawal.

		CTRL		EtOH-WDL 12 h			EtOH-WDL 48 h			EtOH-WDL 14 d		
Global rating		Median	IQR	Median	IQR	*p value*	Median	IQR	*p value*	Median	IQR	*p value*
	Vehicle	0.0	0.0 - 0.0	3.0	3.0 - 4.5	* * *	2.0	1.0 - 2.0	*	0.0	0.0 - 0.5	n. s.
	L-DOPA	0.0	0.0 - 0.0	2.0	1.0 - 2.0	^ ^	1.0	0.5 - 1.0	n. s.	0.0	0.0 - 0.5	n. s.
Individual signs												
Body tremors												
	Vehicle	0.0	0.0 -	0.5	0.0 -	*	0.0	0.0 -	n. s.	0.0	0.0 -	n. s.

			0.0		1.0			0.5			0.0	
	L-DOPA	0.0	0.0 - 0.0	0.0	0.0 - 1.0	n. s.	0.0	0.0 - 0.0	n. s.	0.0	0.0 - 0.0	n. s.
Tail stiffness												
	Vehicle	0.0	0.0 - 0.0	1.0	1.0 - 2.0	* *	1.0	0.5 - 2.0	* *	0.0	0.0 - 0.0	n. s.
	L-DOPA	0.0	0.0 - 0.0	0.5	0.0 - 1.0	n. s.	0.0	0.0 - 0.0	n. s.	0.0	0.0 - 0.0	n. s.
Irritability to touch												
	Vehicle	0.0	0.0 - 0.0	2.0	1.0 - 2.0	* * *	0.5	0.0 - 0.5	n. s.	0.0	0.0 - 0.5	n. s.
	L-DOPA	0.0	0.0 - 0.0	1.0	0.5 - 1.0	^	1.0	0.0 - 1.0	n. s.	0.0	0.0 - 0.5	n. s.

980

Legends

Table 1. Experimental design**.** CTRL alcohol-naïve control rats; EtOH-CHR chronically-EtOH-exposed rats; EtOH-WDL: alcohol-withdrawn rats; L-DOPA: L-DOPA/benserazide administration; DA: dopamine; SCH: SCH23390; Sulp: sulpiride.

Table 2. Rating of behavioral signs of withdrawal. Each individual sign of withdrawal was rated on a 0 - 2-point scale, with 0 representing absence of sign, 1 representing moderate severity, and 2 representing extreme severity. Individual withdrawal sign ratings were then combined to produce a global score. Data are indicated as median and interquartile range (IQR) of n = 8 rats. *** $p < 0.001$; ** $p < 0.01$; * $p < 0.05$ Dunn's post hoc test vs. CTRL; ^^ $p < 0.01$; ^ $p < 0.05$ two-tailed Mann-Whitney U test vs. vehicle.

Figure 1. Alcohol withdrawal disrupts limbic memory formation. Limbic memory was assessed in rats by (a) the emotional object recognition (EOR) test, here schematically represented. Four hours after the cued fear-conditioned learning, rats were put into the central zone of Context A chamber and tested for individual zone preference in epoch baseline (BSL). Afterwards emotional-object avoidance and target-zone aversion were assessed in epoch ON-1 (objects in the arena), OFF (objects removed from the arena), ON-2 (objects in the arena). 12 h alcohol-withdrawn rats (EtOH-WDL) displayed reduced (b) emotional object avoidance and (c) target-zone aversion with respect to alcohol-naïve control (CTRL) and chronically-EtOH-exposed (EtOH-CHR) rats. No significant differences between CTRL and EtOH-CHR were recorded. EtOH-WDL did not show sensory-motor impairment, in terms of (d) total distance travelled (TDT) when video-tracked during the BSL epoch in context A chamber, and (e) tail flick latency following the EOR test. Each bar represents the mean ± SEM of n=8 rats. Each box-and-whisker plot represents the median (horizontal line in the box), 25–75% (box) and min-to-max (whiskers) values of n=8 rats. ***p<0.001; *p<0.05.

Figure 2. Limbic memory disruption was rescued by L-DOPA/benserazide (L-DOPA) after 12 h withdrawal. 12 h alcohol-withdrawn rats administered with L-DOPA (EtOH-WDL +L-DOPA) displayed increased (a) emotional object avoidance and (b) target zone aversion score with respect to 12 h alcohol-withdrawn rats receiving vehicle (EtOH-WDL + vehicle), up to alcohol-naïve control (CTRL) rats' level. Limbic memory disruption was long lasting: alcohol-withdrawn rats showed decreased (c) emotional object avoidance and (d) target zone aversion score following 48 h (EtOH-WDL (48 h) and 14 days (EtOH-WDL (14 d) of withdrawal. Long lasting limbic memory disruption in EtOH-withdrawn rats was not rescued by late stimulation of dopamine transmission. Pre-conditioning L-DOPA is not effective at significantly increasing (c) emotional object avoidance and (d) target zone aversion score

in EtOH-WDL (48 h) and EtOH-WDL (14 d) rats. In contrast, the rescuing effect of early (12 h withdrawal) L-DOPA administration was dose-dependent on both (e) emotional object avoidance and (f) target-zone aversion score. Each bar represents the mean ± SEM of n = 8 rats.

Figure 3. DA increase reverts aberrant structural plasticity in the NAc of alcohol-withdrawn rats. (a) Representative 3D reconstruction of the simultaneous visualization of Golgi-Cox stained MSNs. (b) 3D reconstruction of the simultaneous visualization of Golgi-Cox stained MSNs (red), DA projections (TH+, green), post-synaptic density scaffold (PSD-95, yellow) and long-thin spines (blue) in alcohol-naïve control (CTRL)-, 12 h alcohol-withdrawn rats (EtOH-WDL) - and 12 h alcohol-withdrawn rats administered with L-DOPA (EtOH-WDL +L-DOPA). L-DOPA administration restores the aberrant structural plasticity of the synaptic triad in the NAc of withdrawn-rats. Indeed, L-DOPA (c) selectively expanded the density of long-thin spines to similar values as controls; (d) increased TH levels and (e) produced a complete restoring of the immunolabeling for PSD-95 in the NAc. Each bar represents the mean ± SEM of n = 6-8 rats. ***p<0.001; *p<0.05.

Figure 4. Effects of EtOH withdrawal on LTD formation in rat NAc MSNs. AMPAR-mediated eEPSCs were recorded in single voltage-clamped (-65 mV) MSNs of the NAc shell obtained from the different groups of animals (n of animals, CTRL = 5; EtOH-WDL (12h) = 5; EtOH-WDL (48h) = 4; EtOH-WDL (14d) = 3). (a) Representative eEPSCs recorded before (black trace) and 60 min after (blue trace) LFS paired with depolarization (-50 mV). (b) Scatter plot graph of the changes in eEPSC amplitude in CTRL and EtOH-WDL (12 h, 48 h, and 14d) with data expressed as percent of baseline. (c) The graph illustrates the degree of LTD, calculated by averaging the eEPSC amplitude values measured 50-60 min after LFS and expressed as percent of baseline. The number of cells analyzed is indicated for each group. ***p = 0.0004. (d) The scatter graph illustrates the

distribution of individual values, averaged in (c). Color code is the same as in (c). ***p = 0.0006.

Figure 5. Single acute administration of L-DOPA and bath perfusion of NAc slices with DA restores the hampered LTD formation in NAc shell MSNs from EtOH-withdrawn rats. (a) Representative EPSCs recorded before (black trace) and 60 min after (blue trace) LFS paired with depolarization (-50 mV) obtained in single MSNs from CTRL and EtOH-dependent rats that were tested after 12 h withdrawal. EtOH-WDL rats were subjected to an acute administration of L-DOPA (6 mg/kg, s.c.) and benserazide (6 mg/kg, s.c.), or vehicle, 1 h prior to their sacrifice. (b) Scatter plot graph of the changes in EPSC amplitude with data expressed as percent of baseline. (c) Scatter graph illustrating the distribution of individual data, averaged in (b), calculated by averaging the EPSC amplitude values measured 50-60 min after LFS and expressed as percent of baseline. The number of cells analyzed is indicated in each group and were obtained from 5 animals per group. ***p = 0.0002. (d) Representative EPSCs recorded before (black trace) and 60 min after (blue trace) LFS paired with depolarization (-50 mV) obtained in single MSNs from EtOH-dependent rats that were tested after 12 h of EtOH-WDL. Slices from EtOH-WDL rats were acutely perfused with dopamine (10 μM) 5 min before application of LFS (indicated in green in graph e). (e) Scatter plot graph of the changes in EPSC amplitude with data expressed as percent of baseline. (f) Scatter graph illustrating the distribution of individual data averaged in (e) .The number of cells analyzed is indicated in each group and were obtained from 5 animals per group. ***p = 0.0002. A single i.p. injection of L-DOPA or DA perfusion in slice did not alter LTD formation in NAc shell MSNs from CTRL (g) or EtOH-CHR (h) rats. The bar graphs illustrate the degree of LTD, calculated by averaging the EPSC amplitude values measured 50-60 min after LFS and expressed as percent of

baseline. The number of cells analyzed is indicated in each group and were obtained from 5 animals per group.

Figure 6. Single acute administration of L-DOPA and bath perfusion of NAc slices with DA restore the decrease in NMDA/AMPA ratio in NAc shell MSNs from EtOH-withdrawn rats. (a) Representative EPSCs mediated by NMDA and AMPA receptors recorded in single MSNs clamped at -70 mV (for AMPA) and +40 mV (for NMDAR in the presence of NBQX 5 μM) from the different experimental groups. (b) The graph summarizes the NMDAR/AMPAR ratio obtained from MSNs of the different groups. The number of cells analyzed is indicated in each graph bar and were obtained from 5 animals per group. ***p = 0.0001.

Figure 7. The selective antagonist of D1 but not D2 receptors prevents the restoring effect of DA on LTD levels in EtOH-WDL (12h) rats. NAc slices of EtOH-WDL rats were bath-perfused with DA (10 μM), in the absence or presence of SCH23390 (10 μM) or sulpiride (10 μM), for 5 min prior LFS paired with depolarization (-50 mV). (a-b) Scatter plot graph of the changes in EPSC amplitude with data expressed as percent of baseline. (c) The scatter graph illustrates the degree of LTD, as in graph (a) and (b), and were obtained from 5 animals. The number of cells analyzed is indicated for each experimental group. ***p = 0.0006.

Fig. 8. Single acute administration of L-DOPA restores extracellular DA levels in NAc shell of EtOH-withdrawn rats. (a) EtOH-WDL (12 h) rats displayed lower levels of dialysate DA in the NAc shell, with respect to CTRL rats; L-DOPA/BENSERAZIDE (6/6 mg/kg sc) administration significantly increased DA levels in the NAc shell of EtOH-WDL (12 h) rats, up to CTRL's levels. (b) Notably, L-DOPA induced a larger increase of dialysate DA in the

NAc shell of EtOH-WDRL (12 h) as compared to basal (filled symbol) and to dialysate DA in the NAc shell of CTRL rats expressed as percent of baseline. Each value represents the mean ± SEM of n = 4 rats. ** $p < 0.01$; *** $p < 0.01$

Figure 1

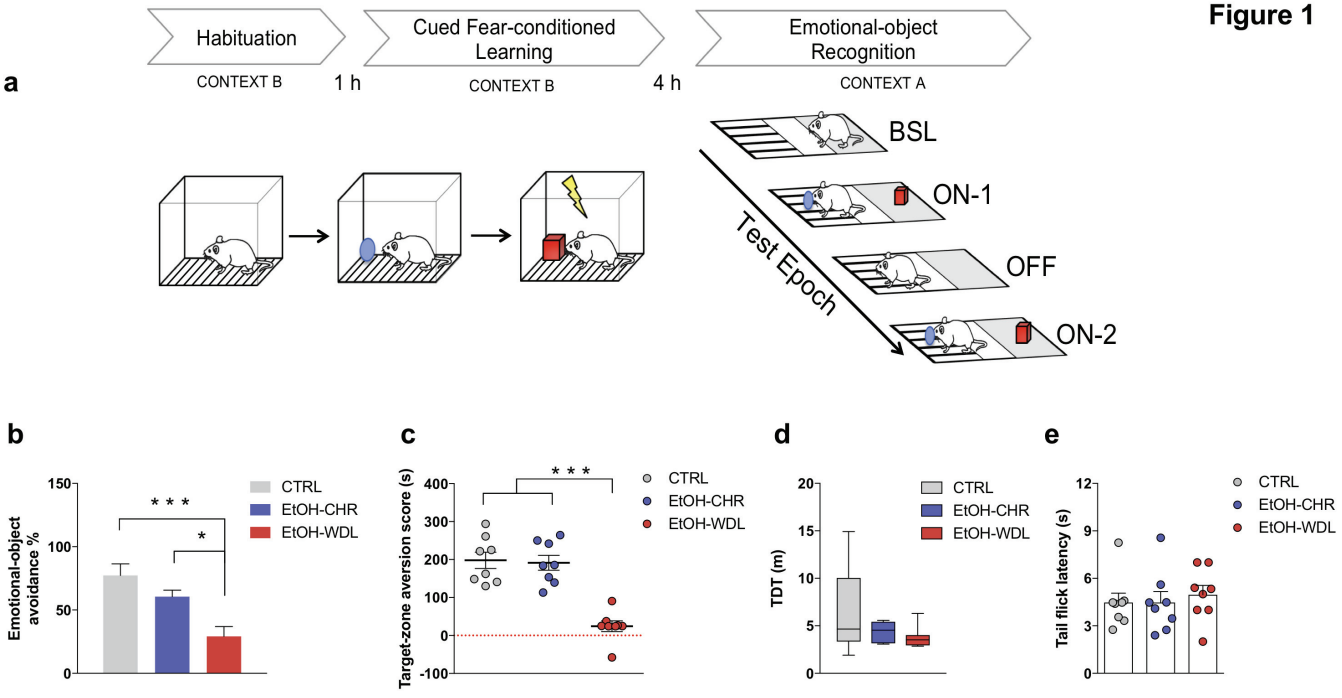

Figure 2

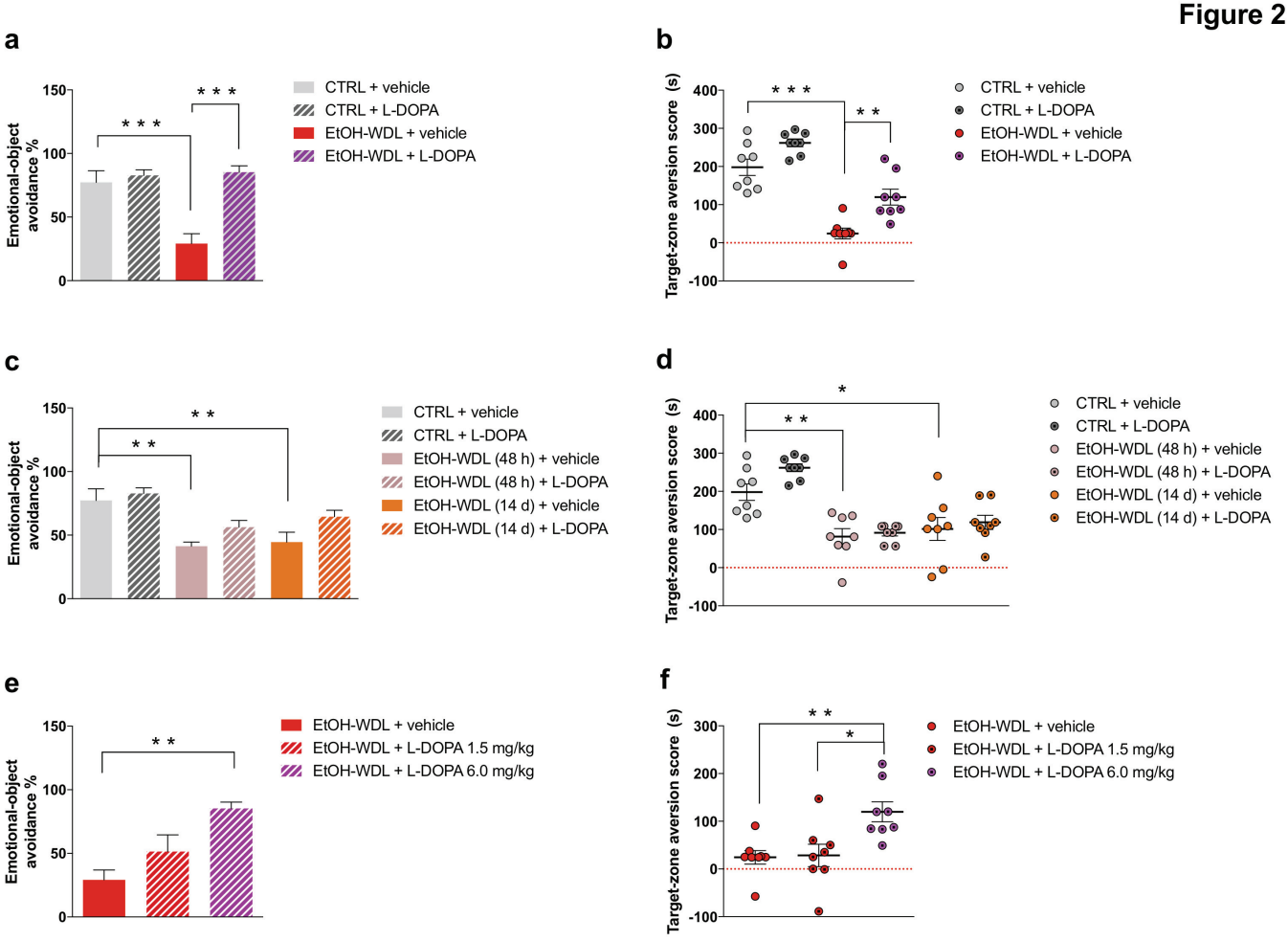

Figure 3

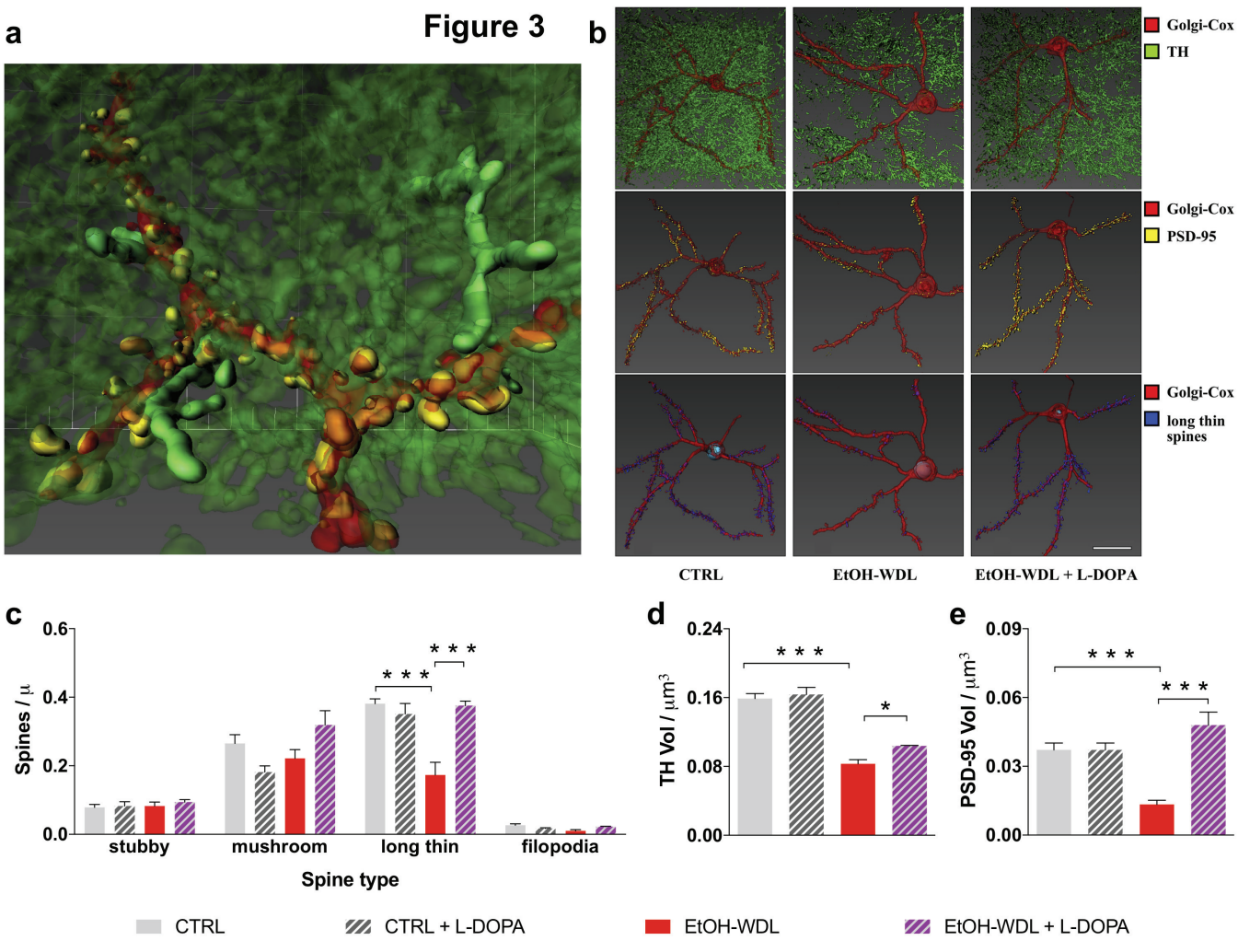

Figure 4

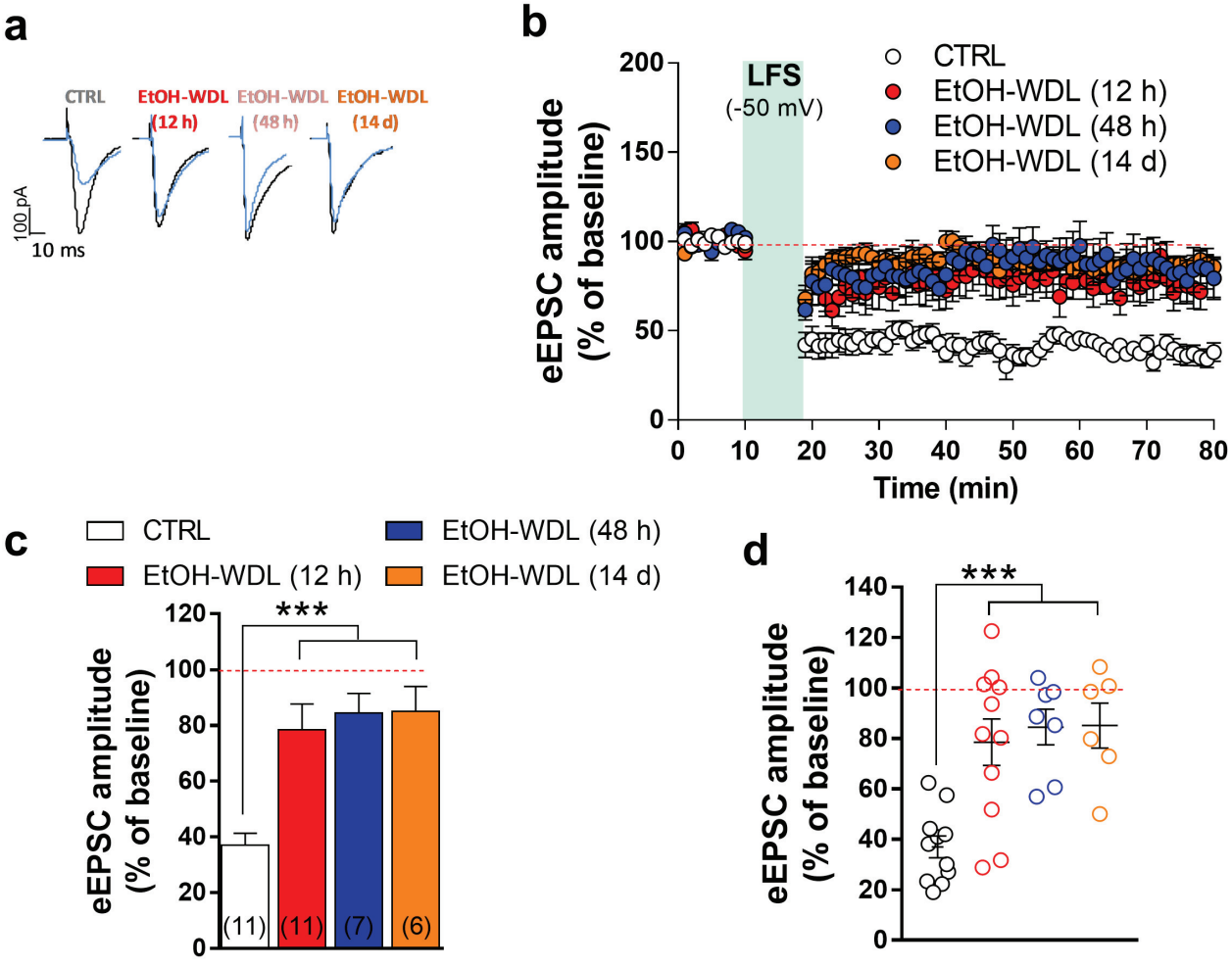

Figure 5

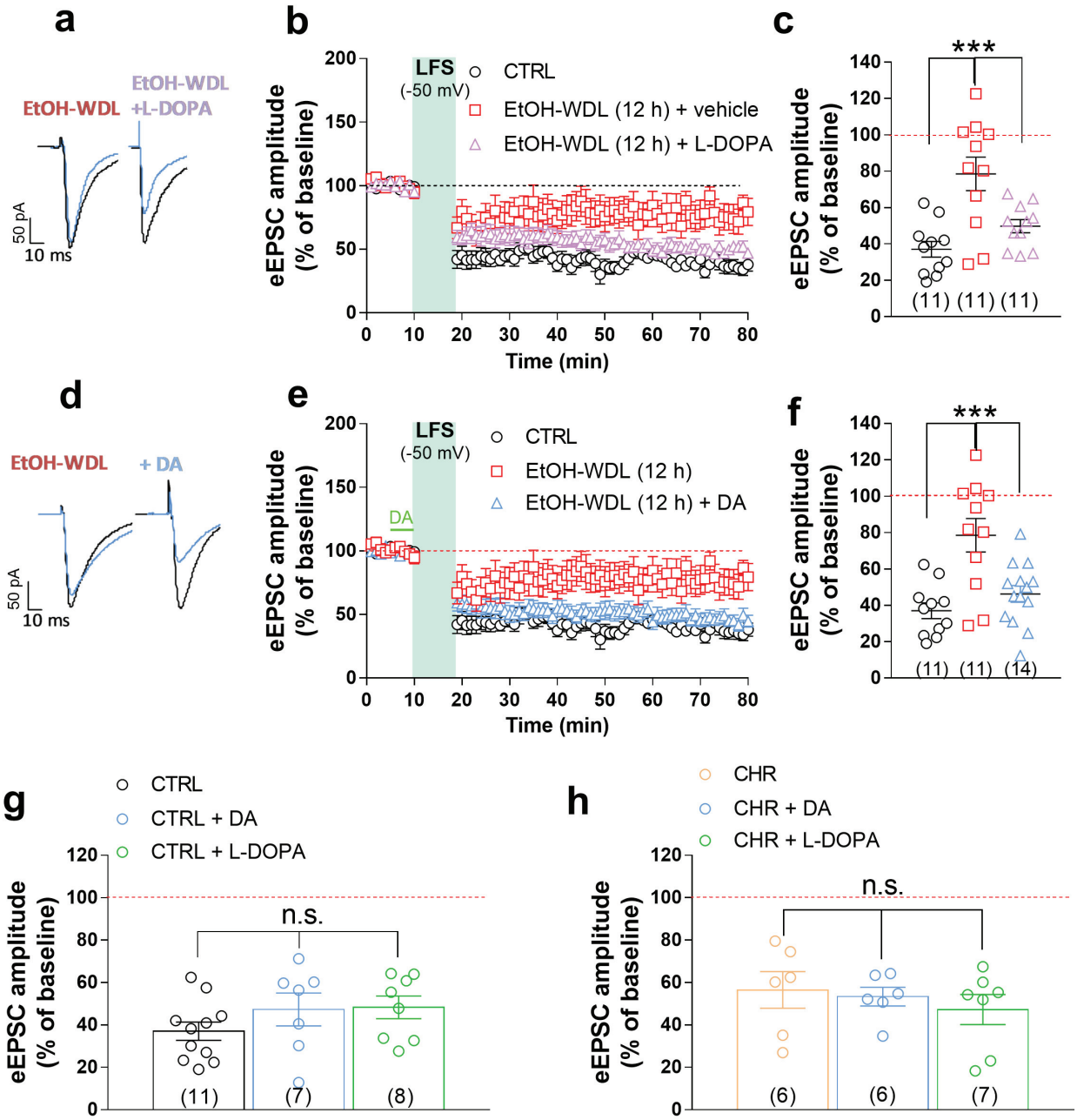

Figure 6

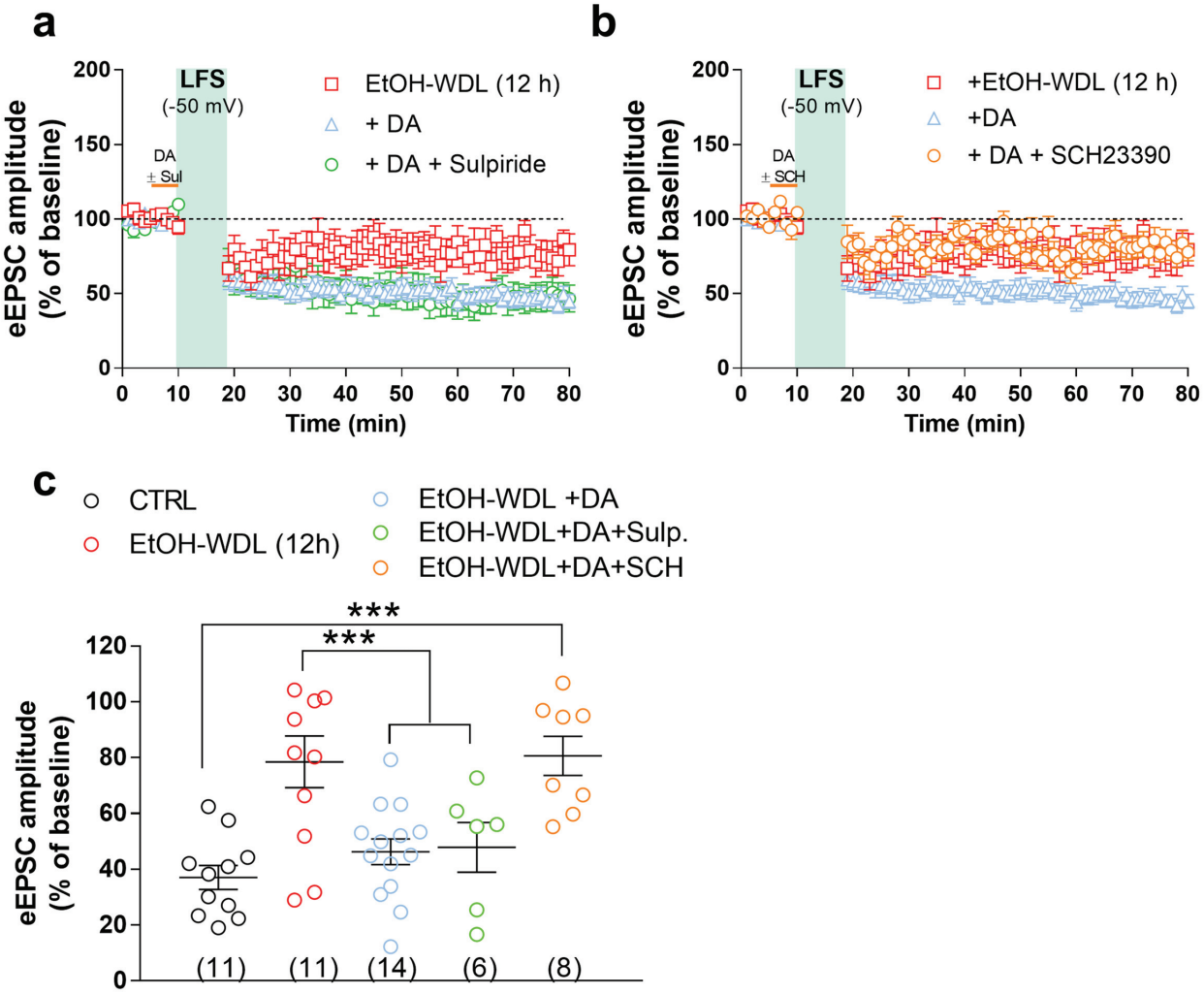

Figure 7

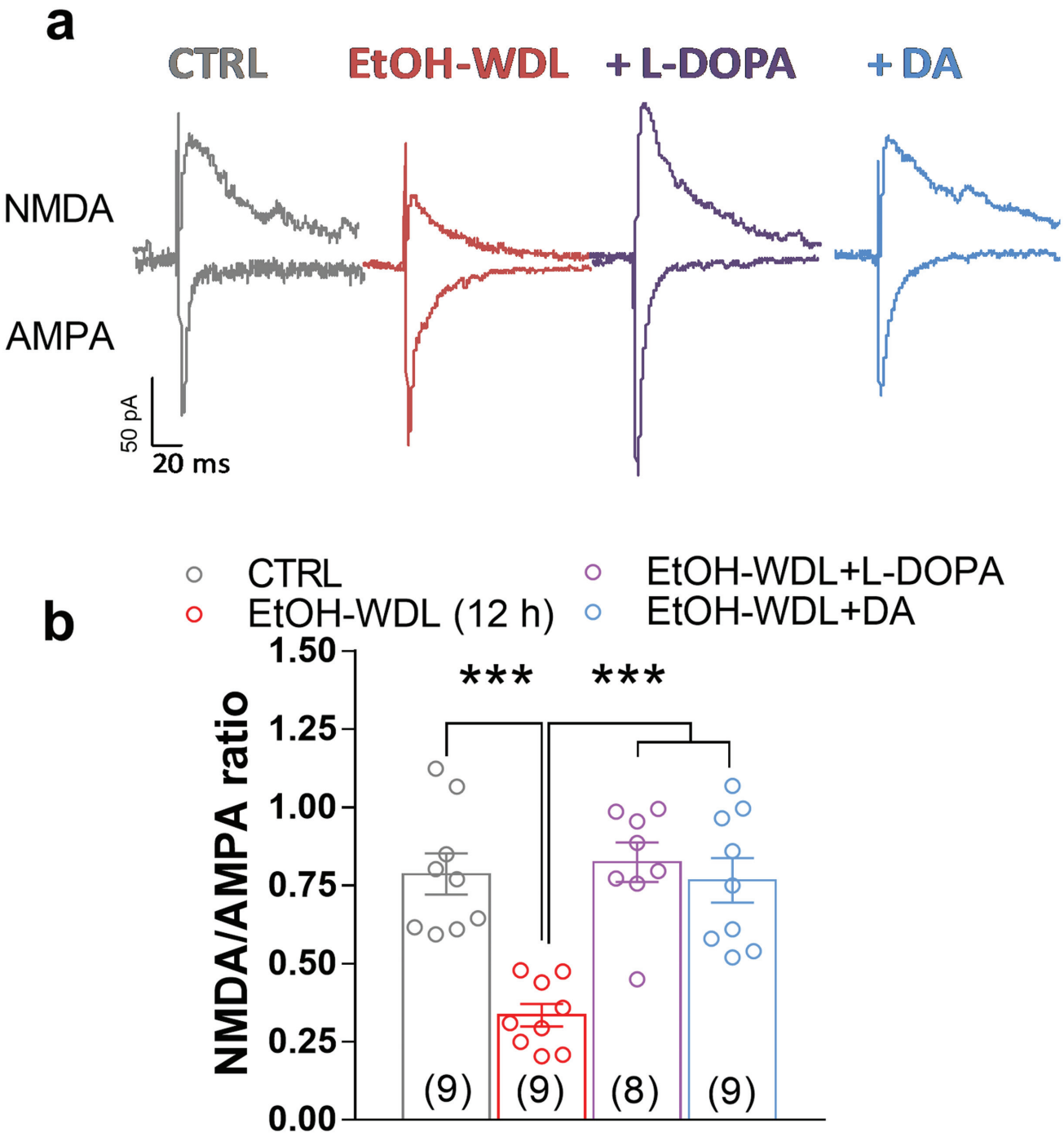

Figure 8